Answers to the Referees of the Production Readiness Review of slats of Stations 3,4,5

28th January 2003

We remind first the questions from the Referees and then answer by grouping some items.

Questions from the referees:

18.01.2002

Report from the Production Readiness Review for the
ALICE muon tracking stations 3 to 5

Held at Nantes 10 and 11 December 2001

Present: SUBATECH Nantes: H.Carduner, M.Dialinas, L.Luquin, A.Tournaire
CEA Saclay: A.Baldisseri, H.Borel, F.Orsini, F.Staley
IPN Orsay: P.Courtat, Y.Le Bornec
INFN Cagliari: M.Arba, C.Cicalo
CERN ALICE: C.Fabjan, H.Taureg

Referees: J.Lefrancois, V.Polychronakos, O.Ullaland

The Production Readiness Review concentrated on the mechanical construction of the chambers, their support and the distribution of services. The electronics were only considered as far as they influence the layout of the slat PCBs. The different aspects of the tracking stations were discussed during 1.5 days.

The referees appreciated the large amount of work done and make the following recommendations:

- The equivalent circuit diagram of a slat should be studied in more detail and compared with measurements on the prototype, this includes the stray capacity between readout lines, between pads and lines, couplings between wire signal and pads, the effect of eventual bypass capacity for wires etc...The amplifiers input impedance should be evaluated and included in the simulation. The grounding, the value of the protection resistor and bypass capacitor should be evaluated. In particular the referees worry that not enough bypass is provided by the intrinsic capacitances of the anode plane and this may lead to an unacceptable degradation of the position resolution. This issue needs to be studied urgently because solutions to the problem may have implications for the mechanical design of the slats.

- The performance of the slat should be checked in a test beam with conditions imitating the foreseen particle multiplicity and particle distribution, it should be studied whether this can be achieved in pion, electron or heavy ion test beam at the SPS.

- The segmentation of the LV distribution should be chosen as a compromise, agreed among the experimenters, between the increase of cost and the tolerable inefficiency in case a shorted electronics component disables a unit; it appeared to the reviewers that a solution such that each slat is independent would seem a better compromise.

- The efficiency across the boundary of the HV segments should be studied when one segment is at ground potential and the neighboring one at nominal HV.

- Aging of a slat should be studied at GIF with an exposure equivalent to the expected dose over the expected lifetime of the experiment.

- The requirements on the calibration system of the FEE need further scrutiny. This may lead to modifications of the slat PCB and is therefore urgent.

- The operating parameters of the slat should be studied in a wider range in order to have a clear view of the performance limitations. The referees suspect that the slat could be operated at lower gas gain without performance deterioration. Lower gas gain would be advantageous from the aging point of view. The requirements on the variation of the gas gain seem unnecessarily tight.

- The referees ask for a review of the admissible tolerances at the different steps in the slat construction.

- The chemical treatment of the NORYL, in preparation of gluing, is being questioned with respect to aging.

- The fixation procedure for wires should be studied further: perhaps one does not have to define the chamber gap at the position of the wire fixation. Perhaps the glue for the wire fixation can be "locked" by a recess in the V-groove.

- It was agreed at the meeting that conductive epoxy is a safer solution for the connection of the wires to the HV instead of the adhesive tape.

- The referees express some worries about the out-gassing, into the sensitive chamber volume, from the RTV seal.

- In view of the distributed production of the slats all conditions, parameters and procedures should be defined clearly in writing. This concerns the specification of the "clean" room environment, the steps of the construction procedure, the selection criteria of components, required tests and checks.

- All relevant parameters should be entered into a database and all parts should be clearly identified.

- One should reconsider the required tolerances, especially on flatness, for the "frame".

- The present overconstrained fixation of slats worried the reviewers. It should be studied whether the slats could not be mounted instead on three support points on the frame.

- The alignment monitoring has received too little attention so far for being reviewed. It is noted, however, that the mounting of components for the alignment

system will have to be defined before the "frames" can be produced.

- The work on cooling appears to be insufficient so far for assuring a safe operation of the slat system. Cooling model calculations should be backed up by a few simple measurements, for example in a 40 cm region of a slat equipped with amplifiers.

Conclusions

The referees consider it essential to further study the topics outlined above before series construction is launched. The results obtained in the studies concerning the above recommendations should be documented before procurement starts. The ALICE Technical Coordination should be informed of the results. It is expected that the studies requested should not interfere in a significant way with the planned procurement.

1 Equivalent circuit diagram and bypass protection (item 1)

1.1 Equivalent circuit diagram

We tried in the PRR document (Chapter 5, section 5.3.2) to understand the measured noise with a simple capacitive model of our detector. We considered only three terms in this model:

- a first term, involving PCB, glue and Nomex capacitance between one pad and the grounded carbon skin,
- a second, involving the glue and Nomex capacitance between the read-out strips and carbon,
- a third, involving PCB capacitance between read-out strip and other pads.

The capacitance obtained with this model for our prototype varies between 5 and 9 pF depending on the length of the read-out strips. If we consider that the noise from our detector comes only from capacitive effects, we then obtain a noise between 580 and 630 electrons. We have taken the characteristic noise of the GASSIPLEX 0.7 μm:

$$\text{noise } (e^-) = 530 + 11.2 \times C \text{ (pF)}$$

Our measured noise in the bending plane is ~ 1 - 1.1 ADC channel corresponding to ~ 1250 - 1350 electrons. The corresponding capacitance would be then: ~ 65 pF.
We obtain a factor of 2 in the noise and a factor between 7 and 13 in the capacitance.
Our model does not reproduce our measurements and we have not succeeded to improve it. We have considered that we measured a good level of noise: we have verified during the beam tests that the prototype was well shielded and we could not lower our noise. The question of electromagnetic compatibility is here not raised: the slat was electrically “isolated” in beam tests. As shown in the test results section (2.1) our resolution plateau is relatively large and we are not dominated by the noise. This can be seen also by the same resolution’s level obtained with lower pad densities (bigger pads) which have little higher noise.

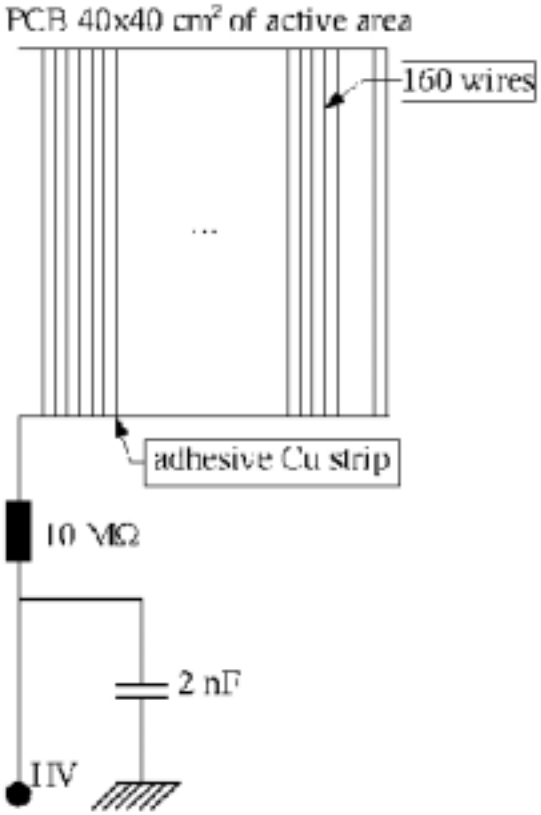

Figure 1.1: HV connection of the 2.4 m slat prototype tested in October 2001

1.2 Bypass protection

1.2.1 Setup used in the 2.4 m prototype tested in October 2001

In the 2.4 m prototype tested in October 2001, all the 160 wires of a given PCB (40x40 cm^{2}active area) were connected together with an adhesive Cu strip to the HV supply. The way how the capacitance and the resistor was connected (see fig. 1.1) could deteriorate the charge measurement, leading to a loss in the position resolution. This is due to the parasitic charge induced in the pads by all the particles coming at the same time. We can estimated this in the following way.

The highest particle density expected in the central part of the tracking chambers of the Stations 3, 4 and 5 is 10^{-2} particles/cm^2 per event, then in the area covered by one PCB we expect $N_{part} \sim 20$ particles coming essentially from the background. The total charge deposited in the PCB will be $Q_{tot} = N_{part} \cdot Q_{mip}$ where the charge of a Minimum Ionizing Particle (MIP) is given by $Q_{mip} = N_{primary} \cdot G \cdot Q_e$, where the number of primary ionizing electrons is taken as $N_{primary} = 30 e^- / cm$ and the typical gain is $G \sim 10^5$, then $Q_{mip} = 0.25\, pC$ using $Q_e = 1.6 \cdot 10^{-19} C$. Let's calculate now the capacitance of the detector to evaluate the energy stored on it. The capacitance per unit length of a "cell" containing one wire is given by (see for instance [1]) :

$$C = \frac{2\pi\varepsilon_0}{\pi l/s - ln(2\pi a/s)}$$

where s, l and a are the wire pitch, the half-gap and the wire radius respectively. In our case $s = l = 2.5mm$ and $a = 10\,\mu m$. Using $\varepsilon_0 = 8.85 \cdot 10^{-12} F m^{-1}$ we obtain for our geometry $C = 8.2\,pF m^{-1}$. The capacitance for the PCB zone (160 wires of 40 cm long) is given by $C_{det} = 8.2 \times 0.4 \times 160 = 525\,pF$.

The induced voltage drop by the particles in the PCB can be then calculated :

$$\Delta V = \frac{Q_{tot}}{C_{det}} \simeq 10\,mV$$

This voltage drop induces a parasitic charge on the pads. For one pad one has : $Q = \Delta V \cdot C_{pad}$, where the capacitance of one pad of surface $S = 5 \cdot 25\,mm^2$ is $C_{pad} = \varepsilon_0 \cdot S/l \simeq 0.5\,pF$ then finally the parasitic charge induced for one pad is $Q \simeq 5\ fC$, which represents 2% of the charge deposited by a MIP (0.25 pC).

Another important point is the pedestal subtraction, that will be done online in the real experiment. Since the 12 bits ADC presently used has a full scale of 3V and the Gassiplex gain is 3.6 mV/fC then one ADC channel is equal to 0.2 fC. If we apply a 3σ pedestal subtraction, like in October 2001 test beam, and we consider an average noise of $\sim$1 channel this leads to minimal charge of 0.6 fC. Then, we keep every pad with a charge larger than 0.6 fC after the pedestal subtraction. The parasitic charge induced has to be kept at a level below 0.6 fC if we don't want to increase the chamber occupancy (fired pads/total pads).

In order to be in the safe side the parasitic charge has to be kept at a $\sim 10^{-3}$ level compared to a MIP, ie at $\sim$ 0.5 fC level.

1.2.2 Possible solutions

1.2.2.1 Proposition of V. Polychronakos

Use an active circuit proposed by V. Polychronakos (fig. 1.2) which acts as a variable capacitor. V. Polychronakos explains how it works *: The active circuit acts as follows: Under normal operation the effective capacitance to ground is 200 pF multiplied by the open loop gain of the operational amplifier. A very large charge will saturate the op amp disabling the feedback mechanism with the result that the capacitance is now just the 200 pF (plus the 400 built in) thus limiting the stored energy.* The idea to have a variable capacitance looks attractive since it avoid the voltage drop and at the same time the stored energy (detector + capacitor) is kept at a low level to prevent chamber damages. Nevertheless this device needs some care, in particular to prevent oscillations and from the point of view of the Slat chambers project seems too late to introduce all the components in the PCB. It uses also active circuits (operational amplifier) which needs also a dedicated power supply. To conclude, it seems to us that the implementation and the setting up of this system will imply significant changes in the current design (mainly PCB's) which will considerably delay the project.

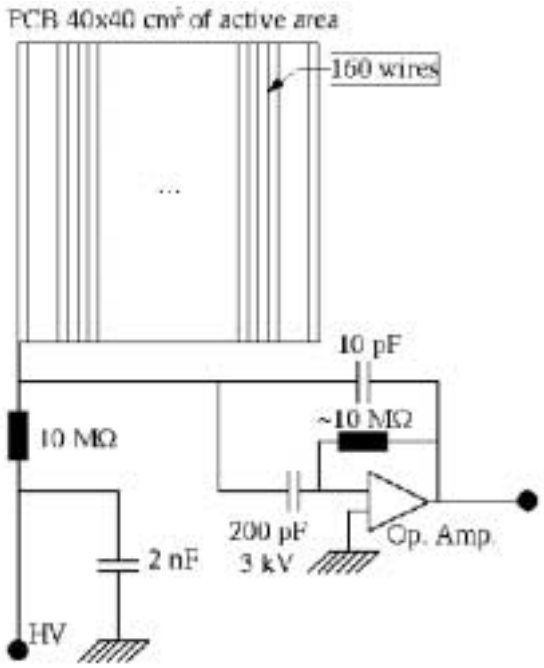

Figure 1.2: Scheme suggested by V. Polychronakos

1.2.2.2 Bypass capacitor and HV supply segmentation

Since the mechanical design is practically final, in particular the spacers, it seems difficult to introduce new components (capacitors, resistors) to do the decoupling wire by wire. Nevertheless, we are investigating the possibility to have a segmentation of the active section of 40x40 cm^2 in 4 or 5 separate HV supplies which will reduce the number of particles per section. Each section should be decoupled from the others using a resistor and a bypass capacitor (fig. 1.3). For example if we split the 160 wires of each PCB in 5 and we use a 2nF capacitor, which is quite standard, then we gain a factor $\sim$20 compared to the calculation presented in 1.2.1. This factor is enough to keep the parasitic charge below the 10^{-3} level and is not destructive for the chamber.

[1] Principles of operation of Multiwire Proportional and Drift Chambers. F. Sauli, CERN 77-09, May 1977.

2 Slat performances (item 7+2+4+6)

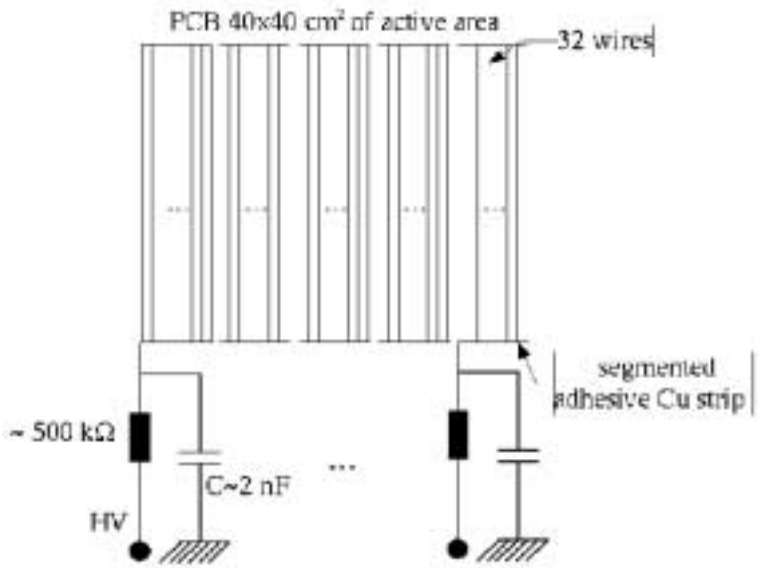

Figure 1.3: Scheme using a bypass capacitor and a segmented HV supply in each PCB

2.1 Analysis results

A detailed analysis of the October 2001 test beam on a 2.4 meter long slat is described in the note ALICE-INT-2002-023.
The pad segmentation is the highest one corresponding to the smallest pads (25 $\times$5 mm^2 for the bending cathode). We obtain a good noise between 1000 and 1300 electrons. A large plateau in resolution and efficiency is observed between 1600 and 1750 V (1600 V was the lowest tested value). The achieved resolution is around 75-80 μm (Gaussian peak) with an RMS value between 120 and 140 μm. The efficiency is 96 % at $\pm$ 1 mm and 92 % at 240 μm (3 σ). Multiple scattering and tracking fit effects are included and the electronics calibration was not available.

Since then, we have explored during July and September 2002 tests, lower HV to optimize the running conditions and observe the limiting parameters. We have also tested on this occasion the other pad segmentations (50 $\times$5 mm^2 and 100 $\times$5 mm^2). In spite of an increase of the noise in density 2 (~1400 electrons) and density 3 (~1600 electrons), the resolution and efficiency are comparable for the 3 densities (Fig. 2.1). The lower edge of the efficiency plateau starts around 1575 V. In running conditions, HV should be set between 1650 and 1700 Volts.

2.2 Angle dependence

Concerning the dependence of the resolution on the incident angle, we observe a usual degradation with a factor of 2 between normal incidence 0 and 10 $^\circ$ (angles expected for the muons in Alice dimuon arm). The corresponding resolutions

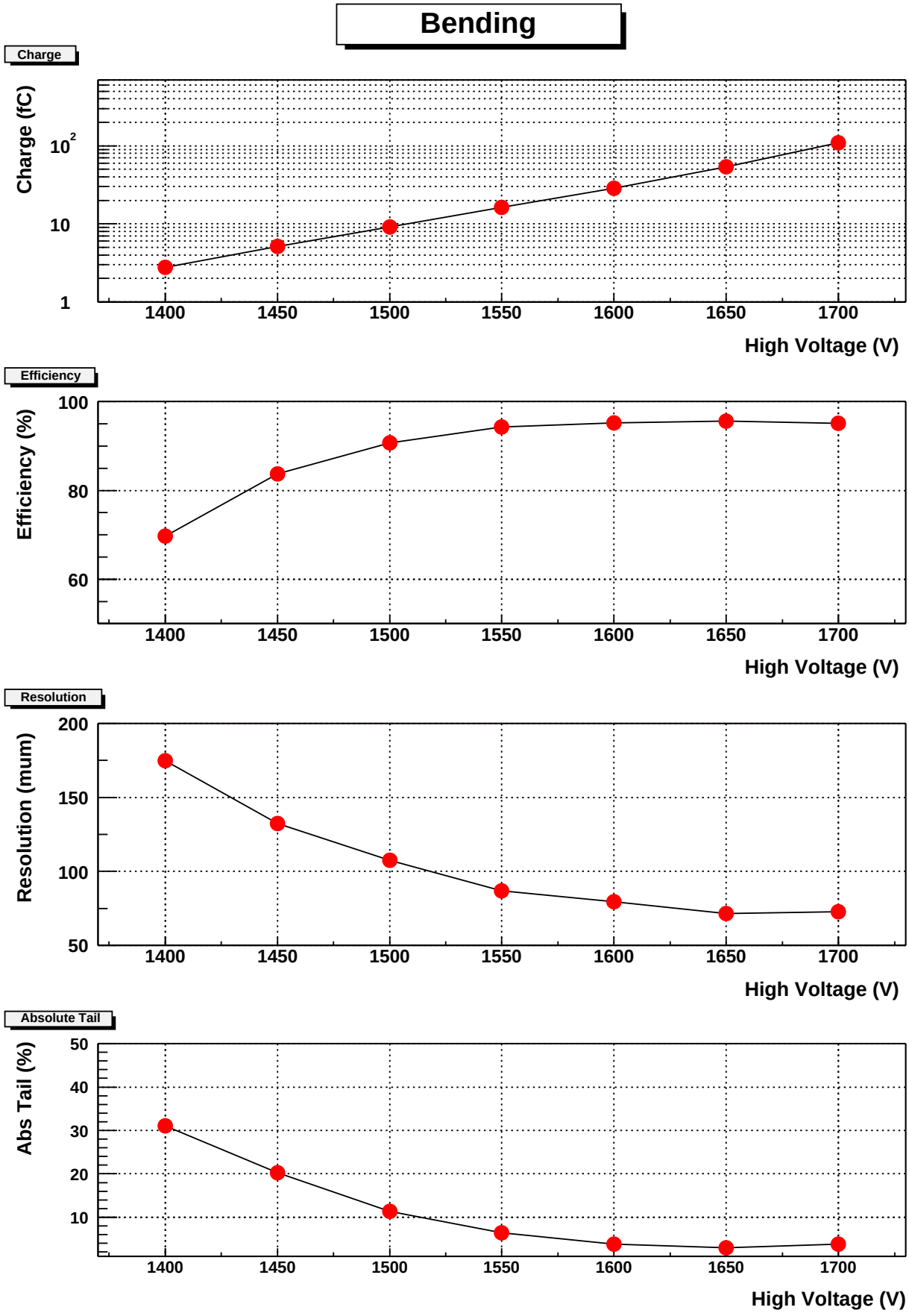

Figure 2.1: Charge, resolution, efficiency ($\pm$ 1mm) and tails (events with residuals between 300 μm and 1 mm) as a function of HV, for segmentation density number 2 (bending pad size 50 $\times$ 5 mm^2).

(Gaussian peak) range from 80 to 150 μm (Fig. 2.2), without multiple scattering corrections (estimated small) and without electronics calibration (not available). We expect to decrease a little bit all the resolutions when this electronic calibration will be set (perhaps even a little more at large angle because of the increased number of pads per cluster involved).

We point out that these resolutions result from a single Gaussian fit of the residuals and we have also to take into account the RMS distribution which also increases with the angles: an idea of the dependence of the RMS value is reflected in the figure 2.2 by the amount of tail (events with residuals between 300 μm and 1 mm).

Pythia code in AliRoot simulations gives an angular distribution of the muons from Υ decay peaked on a relatively small angle of 2.5° with a 3.1° mean value (Fig. 2.3). The background angular distribution is flatter.

To have an idea of the consequence of the poorer spatial resolution on the Υ mass resolution, we have taken in AliRoot, the residual distributions obtained from testbeam. The procedure is to use the GEANT hits and affect them a degraded resolution as a function of the incident angle. With or without background, we hardly see any effect when taking or not into account the angle effect, neither on the resolution (change from 97 $\pm$1.5 MeV (no angle, no background) to 100 $\pm$1.5 MeV (angle, no background) and 102 $\pm$1.5 MeV (angle, nomina

l background)) nor on the reconstruction efficiency (82.7 $\pm$0.5 % to 82.1 $\pm$0.5 %). I remind that the mass resolution is, as usual, the result of a Gaussian fit to the reconstructed Υ mass distribution between 9.3 and 9.8 GeV/c^{2}and the efficiency is obtained from events with mass between 9.17 and 9.77 GeV/c^2. When using a full simulation, the finding and deconvolution of clusters could be a little more affected by the poorer spatial resolution when considering Υ with background. This step is more difficult to simulate and is not yet implemented. Nevertheless, we have made a similar study when using realistic chamber responses from test beam and have not seen substantial effects (see 2.3).

2.3 Remarks on resolution and efficiency obtained

- The detection efficiency with at least one cluster in the chamber is 99.9% at 1650 V.

- The 92 % position reconstruction efficiency value at 3 σ could be considered as low, but we find the same kind of results for station 1 and also in the literature; for example, the ATLAS muon spectrometer CSCs show an inefficiency for one layer between 5 and 10 % (ATL-MUON-2000-005).

Nevertheless, we tried to understand these results by simulation:

- First, we simulated the T10 test bench (with the Silicon trackers) in the AliRoot environment and tried to reproduce the measured spatial residuals.

The residuals are never Gaussian: even if we choose one charge in the Landau distribution, then spread this charge on the pads according to a Mathieson distribution and finally reconstruct the position either with a Mathieson fit or a center

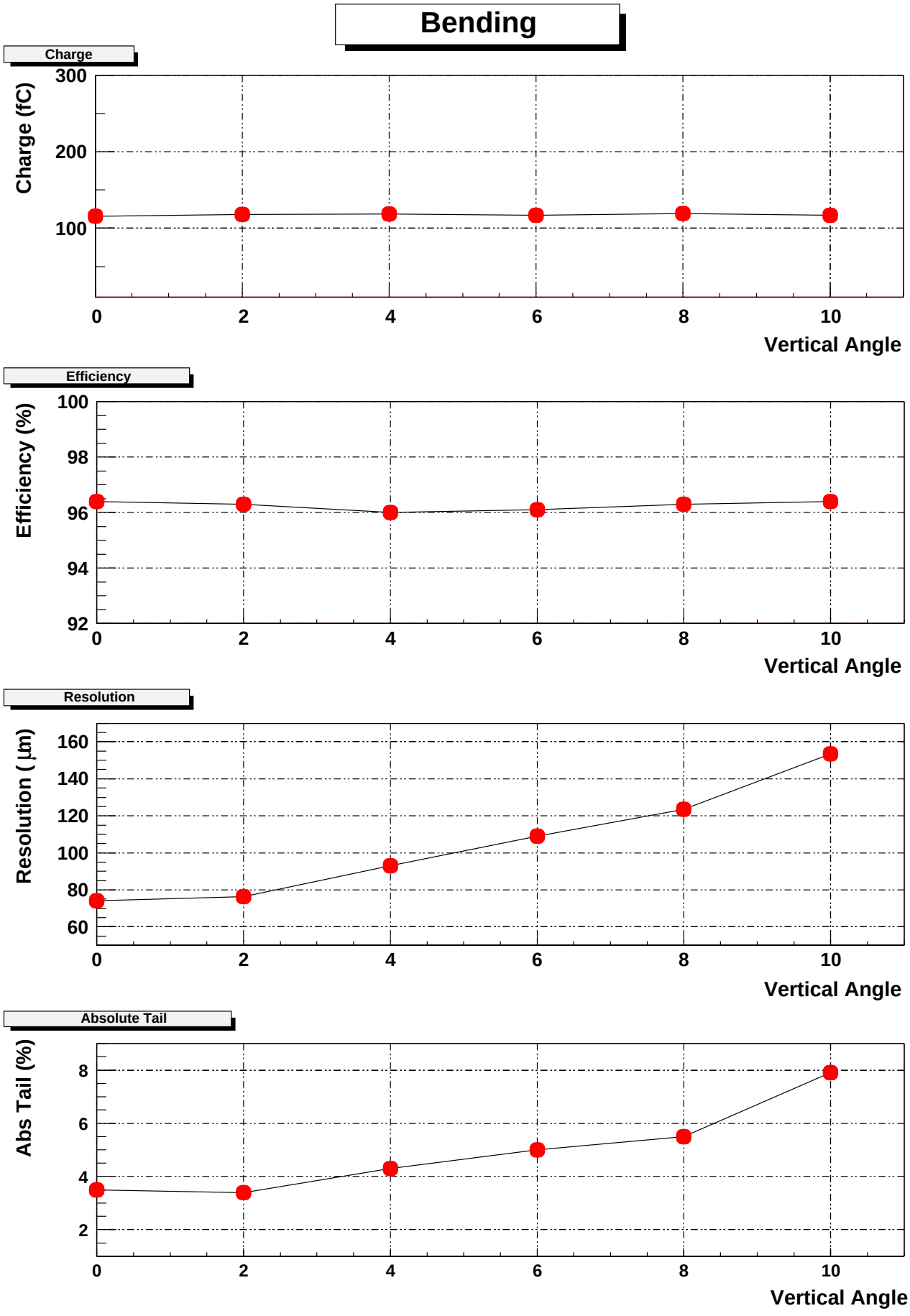

Figure 2.2: Cluster charge, efficiency (± 1 mm), resolution and tail as a function of the tilt angle with respect to the anode wire, for the bending plane. The null value corresponds to normal incidence onto the wire.

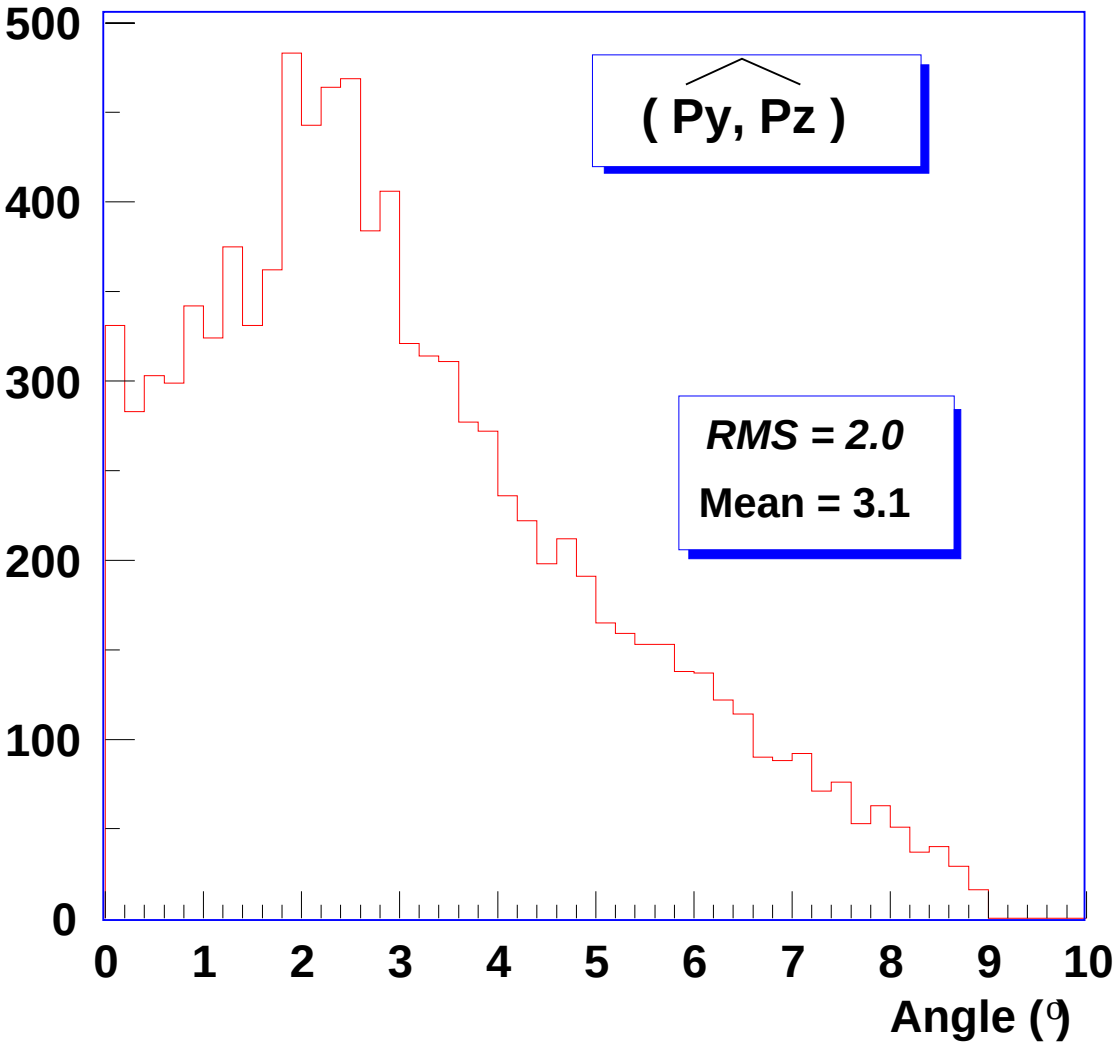

Figure 2.3: Angular distribution of the muons from ϒ simulated by Pythia code.

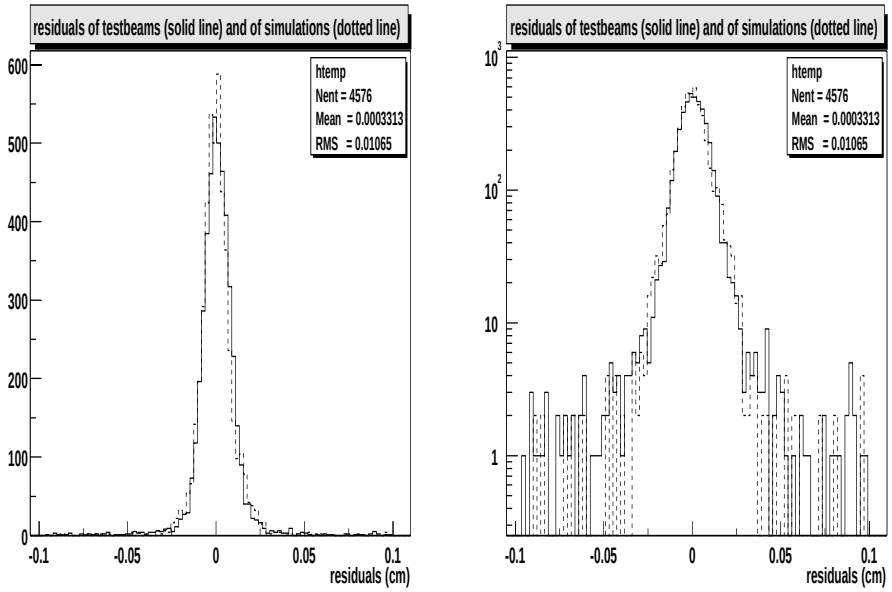

Figure 2.4: Simulation (dotted line) and test beam results (solid line) residuals comparison (left: linear scale; right: log scale).

of gravity, the residuals have already some little tails. Of course, considering the whole Landau distribution will increase the tails, as well as the effect of the noise.

We have now to adjust the parameters, noise taken from the beam test (7 GeV pions) and gain; usually, GEANT gives the energy lost by ionisation in the gas, from which we can deduce the number of primary electrons; then for each single electron, the charge after the avalanche multiplication follows a distribution depending on the gain. Here, as GEANT does not give the good energy loss, we fix the expected number of primary electrons and adjust the gain to obtain the same charges and multiplicities (hit pads) as for the test. The obtained residuals (including multiple scattering as in test beam) are too narrow, giving a good efficiency at ± 1 mm but not the right one at 3 σ. We have to spoil the resolution: increasing the noise by 50% degrades the efficiency but the residual shape is not well reproduced with a narrow Gaussian peak on a large Gaussian distribution. A second approach is to fit the simulated pad charge distributions, to determine the position, with a Mathieson where the parameter K3y (related to the extension of the charge on the pad in the y direction) is different from the one used to spread the charge. This new K3y value is obtained from the test beam results when we fix the position obtained and look at the dispersion of the K3y values around the favored one used for the spreading. This method gives similar results for the residuals, resolution and efficiencies than in the test beam analysis (Fig. 2.4).

- In a second step we look at the effect of the spatial resolution and efficiency on the mass resolution and the reconstruction efficiency of the upsilon, with the full dimuon AliRoot simulation including the parameters obtained above.

	Bkg0	Bkg1
σ (MeV) old	96 ±1	115±2
σ (MeV) new	98±1	121±2
ε (%) old	80 ±1	73±1
ε (%) new	79±1	71±1

Table 2.1: ϒ mass resolutions and reconstruction efficencies obtained with the fast simulation.

A first result (see table 2.1) has been obtained by A. De. Falco with the fast simulation in which the residual distributions were taken from the test beam. Hardly no effect on the upsilon mass resolution nor on the reconstruction efficiency was observed with or without background.

With the full simulation, compared to the results obtained with old parameters which was a little too optimistic concerning the spatial resolution and efficiency, we obtain for upsilon without background, almost the same mass resolution (change from 97 ± 1.5 MeV to 100 ± 1.5 MeV) with the same reconstruction efficiency of 82% (from 82.7 ± 0.6 % to 82.0 ± 0.6 %). The resolution is largely dominated by the role of the absorber.

The background could affect differently the fast and full simulation: the finding and the deconvolution of clusters, which is not present in the fast simulation, can be dependent on the background level.

When taking into account the nominal background in the full simulation, the efficiency is very little affected from 73.3 % to 72.4 % with a 0.6 % statistical error. As a conclusion, the absorber has a dominant role and the ϒ mass resolution and reconstruction efficiencies are not changed when considering more realistic chamber responses. Without background, the mass resolution is around σ =100 ±1.5 MeV and the reconstruction efficiency ε = 82 ± 0.6 %. With a nominal background, σ = 120 ±2.4 MeV and ε = 72 ±0.6 %. Figure 2.5 shows the ϒ mass distribution generated with 5000 ϒ and one nominal background.

2.4 Efficiency across the boundary of HV segments

To study the behaviour of a slat, when the HV of two adjacent PCBs drops down, we made a simulation by using Garfield program. We calculated the gain[1]for a CSC at 1650 V.

In Fig. 2.6 results are shown. In the x axis two wires of one PCB (at HV=0, circle symbol) and seven wires of the adjacent PCB (at HV=1650V, triangle symbols) are shown. In the y axis the corresponding gain value is reported.

[1]With gain we mean the number of electrons produced by a primary electron during the multiplication process.

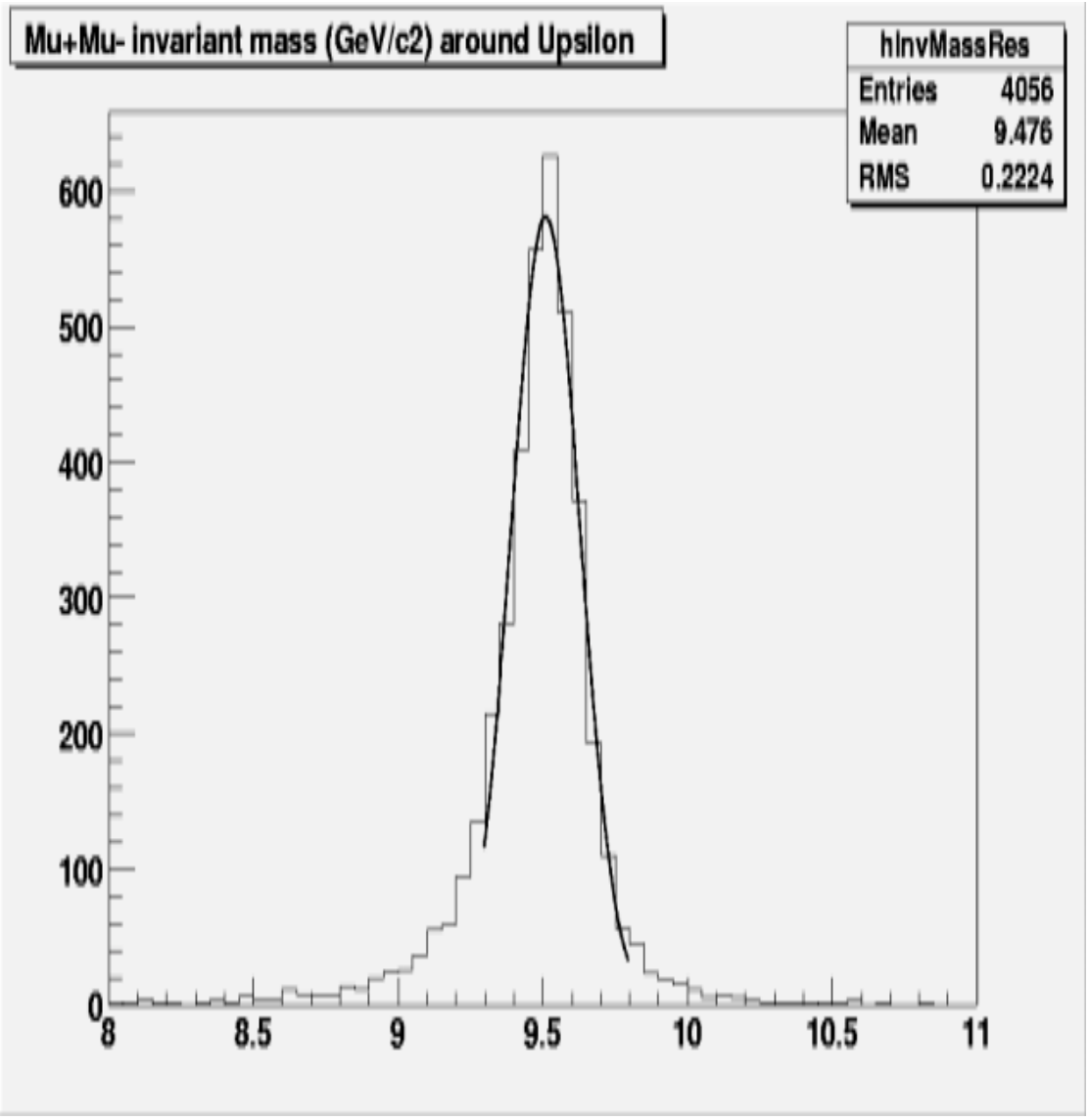

Figure 2.5: Mass spectrum for ϒ resonances with nominal background

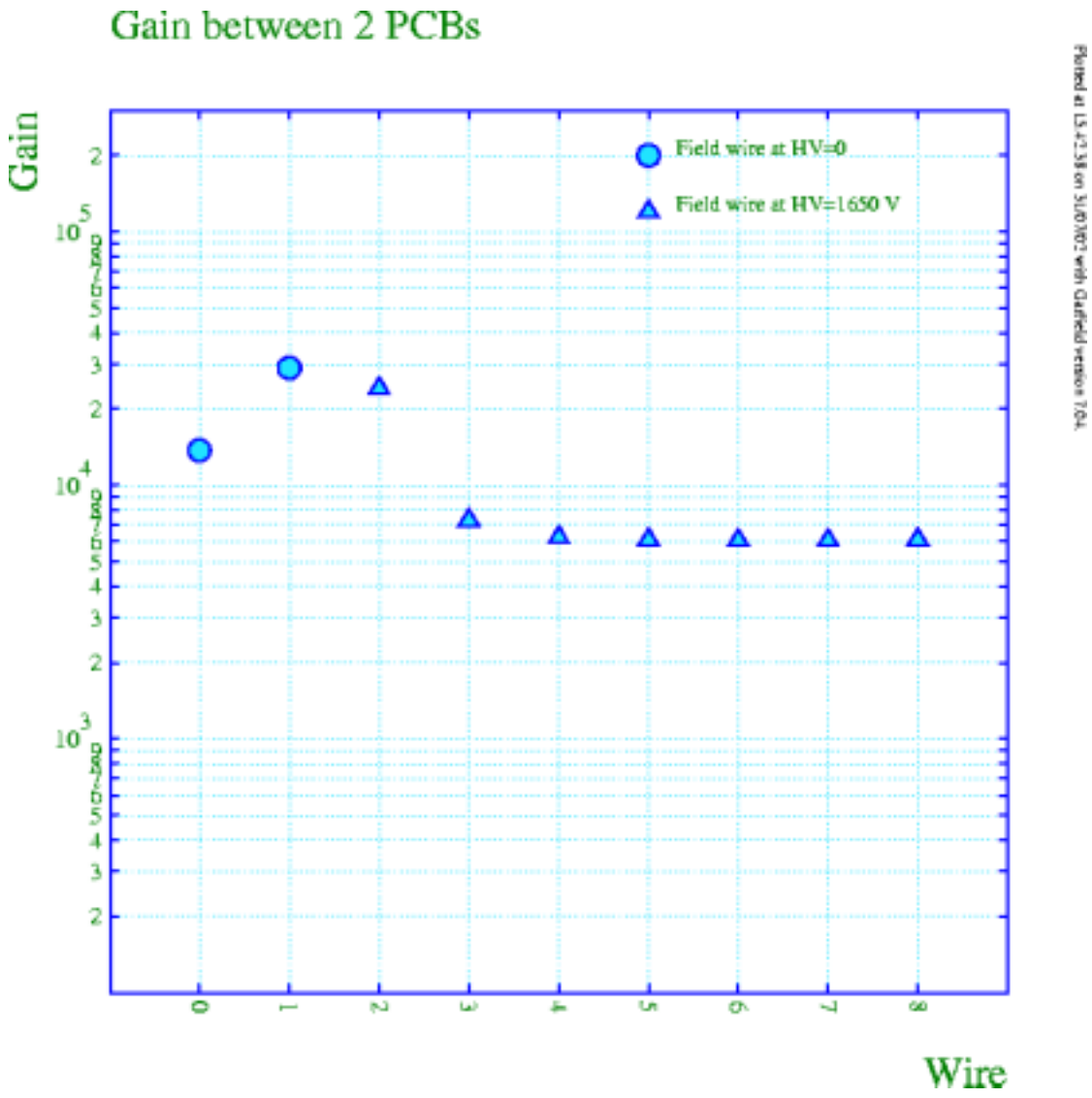

Figure 2.6: Gain value between two PCBs when the HV of one PCB is zero (circle symbols). In the x axis the wire number is displayed.

A not uniform behaviour is expected in this region since now the electric field, between the two PCBs, is higher than in the middle of the chamber. A gain increase is therefore foreseen in this region. As shown, the active region in which the gain is not uniform is less than 5 mm wide. This value seems to be not so crucial, if compared to the 400 mm region inefficiency. The validity of these simulations must be confirmed by experimental tests.

Nevertheless, we have already run with one PCB off on the 2.4 m long prototype in October 2001, without observing discharges.

2.5 Multiparticles effects

Two main problems can occur due to multiparticles:

One is the global "cross-talk" effect coming from the little variation in HV due to the charge deposited by the particles on the anode plane, which induces a uniform charge on the cathode planes via an anode-cathode capacitance. This point is treated in section 1.2 by HV segmentation and an appropriate decoupling capacitor value to decrease the cross-talk to 10^{-3} in order to not degrade the resolution and even more to avoid a larger occupancy.

The second is related to the ability to reconstruct good clusters in a multiparticle environment and is more related to software improvement.

An SPS test has not yet been realized mainly for two reasons:

First we were not ready for this kind of multiparticle test because it needs good trackers with a sufficient area. Since recently, the X5 beam seems more easely available and we plan to use it in 2003, but for "single " particle test.

2.6 Electronics calibration

As already mentioned, all the tests were previously achieved without electronic calibration. Of course, this one is needed to reach very good resolution and in that case the precision on the calibration must be high, of the order of 1%.

As also already mentioned, the MANAS chip is not yet available so slat and especially PCBs have not been tested with the final electronics. Moreover, the way to calibrate is different between GASSIPLEX and MANAS.

The start of the PCB procedure for the production is waiting for a complete read-out of a slat, with MANAS chips and their calibration. As few MANAS arrived finally at the very end of 2002, the calibration could be tested in the first trimester of 2003 (handling of the signal...) but the real impact of this calibration on the spatial resolution will wait the foreseen test beam in spring 2003.

3 Aging due to radiation (item 5)

The total radiation dose expected in a chamber, for 10 years of LHC running, is in most cases lower than 100 rad (1 Gy) (see TP: CERN/LHCC 95-71, LHCC/P3 15 dec. 1999) but can reach in a pessimistic scenario 3 Gy in pp runs in the first station.
We have estimated the charge accumulated on the anode wires during this period of time:

The hypotheses are:

- gas : Ar(80)-CO_2(20)
- gain : 5. 10^4
- the anode wires are grouped by 160 (corresponds to 1 PCB $\equiv$40 cm)
- we consider the maximum density of particles expected in a chamber, for one collision: 5. 10^{-2}cm^{-2}; it corresponds to the peak value in station 1 for a central Pb-Pb collision at dN/dy = 8000 with, in addition, a safety factor of 2. It takes into account charged particles but also gammas and neutrons for which the sensitivity of the CPC is 10^{-2} and 10^{-4} respectively.
- the number of collisions expected in Pb-Pb during 10 years is : 4. 10^{10}

For Pb-Pb collision only, the charge accumulated by wire length unit (for 10 years) is then: $Q_{max} \simeq 5$ mC/cm .

If we consider also the p-p and Ca-Ca runs we obtain:

$$Q_{max}^{Tot} \simeq 30 mC/cm$$

According to the literature, this value is lower enough to not create prejudices: a report “Summary and Outlook of the International Workshop on Aging Phenomena in gaseous detectors” of a workshop held at DESY (Hamburg) in October 2001 (hep-ex/0204005v1 4 Apr. 2002) concludes that up to 1 C/cm of charge deposited there is no aging effects in Ar-CO_2.

Anyway, a test is foreseen at GIF, to test the aging of different components of a slat.

We will expose a slat to a ^{137}Cs gamma source of 660 KeV. The average energy deposited in the gas chamber is expected around 8.5 keV. The flux and time needed for a 1 Gy dose is then (taking into account a CSC sensitivity to gamma of 10^{-2}):

$$\phi.t \simeq 6.6\,10^{10} cm^{-2}$$

The GIF flux can be adjusted between 10^3 to 10^6cm^{-2}.s^{-1}.

We could not achieve this test in 2002 but ask for a GIF period at the beginning of 2003. We would mostly read the anode signal of a small slat during the exposure in order to control the gain.

Another worry is the neutron fluence expected in the dimuon arm: it varies between 10^8 to 10^{11}n.cm^{-2}(for neutron energy > 20 MeV) with a maximum value in station 1. The electronics could especially suffer of this fluence. We are thinking about a neutron test and investigating at the Louvain-la-Neuve facility: fast neutron beams in the 20 to 80 MeV range are available and were developed for LHC test, mainly for CMS with a maximum flux of 10^{10}n.cm^{-2}.s^{-1}. The desirable fluence for our test could be reached in few minutes. Detailed tests have to be defined.

4 Slat construction (item 8+9+10+11+12+13+14)

4.1 Review of the admissible tolerances at the different steps in the slat construction (item 8)

4.1.1 Sandwich panels

- The required flatness needed is 150 μm/m.
- Control of panels flatness will be made with a dedicated Planeimeter Tooling, designed, built and operated at Subatech Nantes.

4.1.2 PCBs.

Etching

- The tolerance needed on the etching of the whole active area along the x direction, namely the distance between the first and the last pad borders on this direction, is $\pm$ 75 μm for a size of 399,500 mm.
- Control of PCBs etching is made with a Coordinate Measurement Machine + an Optical Device (3D measuring machine). Both toolings are installed in Cagliari.

Border cutting

- Tolerance needed on the nominal width is $\pm$ 85 μm for a size of 399,975 mm.

- Tooling for border cutting has been studied and built by PNPI in Gatchina, and shiped for using in Cagliari.
- Control of cuttings is made with the 3D measuring machine, installed in Cagliari.

Holes Punching

- Tolerance needed on the holes position is $\pm$ 10 μm for a size of 230 mm.
- Tolerance needed on the holes diameter is -0, +10 μm.
- Tooling for punching has been studied and built by PNPI in Gatchina, sheeped for using in Cagliari.
- Control of punching is made with the 3D measuring machine too, installed in Cagliari.

Connectors soldering

- Controls : for the Electric Continuity tests, a dedicated tooling has been studied, built and installed in Cagliari.

4.1.3 Spacers

- Tolerances on several dimensions are measured by producer and given at Subatech-Nantes.
- Material quality certificates are given by producer at Subatech-Nantes.

4.1.4 Wires Planes

- Material quality certificates are given by producer at CEA-Saclay.
- Wiring Machine : all the new devices will be controled before the production, by measurements of a dedicated wire plane.
- Strength of the wires is given by the machine and it is conserved by gluing (or something else) on the transfer frame.

4.2 Chemical treatment of Noryl (item 9)

There are 2 options:

Chemical treatment of Noryl is used before gluing:
in order to achieve a good adhesion, Noryl needs to be chemically treated with a sulfa-chromic solution : 45g dichromate Na + 885 g H_2SO_4 + 70 g H_2O, to be processed at 20°C with a process time of 20'. It is foreseen to use the vacuum cleaning

process to remove remaining chemical agents (Mathewson cleaning process). As this process allows to perform very low outgassing rate, it is a way to remove components trapped at surface of materials which may induce aging in wires chambers under significant flux of particles.

Chemical treatment is not needed.

It appears that, in this design, shear stress induced by mechanical loading at different interfaces is far below ultimate shear stress of standard 2011 araldite epoxy glue which is 20 Mpa.

Shear stress is 0.098 Mpa at interface between PCB and Noryl spacer.

Shear stress is 0.39 Mpa at interface between V groove of glue and Noryl spacer.

Shear stress is 1.27 Mpa at interface between glue and tungsten wire.

Taking these datas into account, since early June 2002, long term tests in order to qualify non chemical treated Noryl interface, are conducted with respectively 0.19 Mpa (roughly 2 times real loading) and 2.25 Mpa (roughly 23 times real loading) at interface between Noryl sample and epoxy-glass sample.

First conclusions are, that today we no more expect to process chemical treatment on Noryl spacers.

4.3 Fixation of the wires and chamber gap (item 10)

Experimental tests conducted for item 9 show that epoxy glue does not need to be locked, taking into account the low shear stress between V-groove and epoxy glue. In parallel, since January 2002, long term test is done about the reliability of gluing wires in V shaped Noryl grooves with 200, 400, 500 g stretching load of Ø =70 and 100 μm wires (for a nominal 30-40 g value).

In conclusion, the glue does not spread neither along the wire direction nor in the perpendicular one. An inspection and if necessary cleaning of the top of the spacer is done when gluing, in such a way that the gap remains well defined.

4.4 HV wire conduction (item 11)

The study is under way:

The easiest option is to use silver filled epoxy, reliable, known, but not cheap.

A second option is to use silver filled varnish: mechanical and thermal tests have been recently realised to control that this varnish will not crack and consequently that the electrical continuity will be insured.

Other options are to use graphite, or nickel, or copper filled epoxy. This is a cheapest way that former one, but not easy to set up at a good viscosity, and for repeatability of properties. Test with different solvents are on the way.

In conclusion, we tend to the silver filled varnish solution which is easiest to handle.

4.5 Out-gassing from RTV seal (item 12)

Out-gassing from RTV seal may be dangerous at high particles' rate. From litterature, it seems that critical level of deposited charge for aging process is 1C/cm wire when operating wire chamber with Ar/CO2 mixture. As shown in chapter 3, the expected charge deposited during 10 years of LHC running is 30 mC/cm, below the critical level.

If one fears that real deposited charge is higher than expected value, we have to take into account out-gassing properties of some organic materials.

- PVC which is now forbidden for gas piping features a TML (total Mass Loss) of 15.59%
- Araldite glue, widely used in detectors (and in slats) features a TML of 5.18%
- RTV162 which may be use for sealing features a TML of 1.59%
- RTV160 which is used today for sealing has a TML of 2.7% after 1 week cure, and an additional 0.4% after bake-out (4 weeks at 45°C or 2 weeks at 60°C) which suggests that main part of volatiles are released during cure process. Main outgas product is methanol and we do not think that methanol is dangerous for the aging point of view. There is also 0.42% of volatile condensed material which probably contains silicon compounds like SiO_2 which effect on aging has to be tested at GIF.
  As said in section 3, we plan to control the gain of a 40 $\times$40 cm^2 prototype during GIF tests, by reading the anode signal.

If we think, or if experimental test at GIF shows, that these out-gassing values are too high, General Electric (supplier of RTVs), suggests to process a bake-out, like vacuum pipes, but at a lower value in order to outgas the organic materials before using at CERN. Bake out may be from 2 weeks up to 4 weeks at 45°C upt to 60°C (as indicated above).

4.6 Procedures and specifications for slat production (item 13)

4.6.1 Specifications of the clean room environment

Few meetings have been organized between the four institutes (INFN-Cagliari, Subatech-Nantes, PNPI-Gatchina and CEA-Saclay) in order to determine the characteristics of the future slats assembly rooms. A document has been written on this subject and it is presented in Annex : 'Specifications of the clean room for the wire chamber assembly of Stations 3-4-5 of the Alice experiment ' version 4-14/06/02.

The first part of the document describes the specifications of the clean rooms as below :

A cleanliness class 100 000 and the following specifications seem to be well sufficient to assemble wire chambers in good conditions. We are particularly sensitive to dust, of filament type, with typical size of 500 μm to 2500 μm (~ the half gap of the wire chamber).

Global specifications required for the clean room size are :

- Minimum area = 50 m^2. Maximum area = 100 m^2. Minimum height. = 2.50 m.
- At least 1.20 m room around the assembly table (marble) is required.
- Cleanliness class = 100 000 (US 209B standard).

The specifications required for the clean room are the following :

The clean room must be in overpressure. Overpressure = 0.1 mbar. Overpressure is important to prevent from input of dust during all phases where the slat is still opened. Overpressure can be obtained easily with fans (airflow = 0.3-0.6 m/s) and a system of filters (pre-filter at input and final filter at output). Institutes have to take care with the air distribution : a distributed exhaust in the whole length of the room is ideal. Moreover, the machine of air distribution must not be noisy ! Rough sealing is required too on doors and windows in order to keep differential pressure.

Dust counters are very expensive (4-11.8 kEuros). Consequently it is not realistic to have one dust counter for each institute. Search is on the way to find a cheaper device.

Temperature : regulated at $21^\circ C \pm 3^\circ C$ (a thermostat is required). Maintaining a constant temperature is important during the gluing phases, especially during the gluing phase of the PCBs.

Humidity : 50%-60% (a hygrostat is required). A value close to 50% or less is required for the curing phase of the epoxy resin, whereas a maximum value of 60% is required for the curing phase of the RTV Silicon resin.

Walls : anti-dust paints if possible.

Ground : anti-dust paint on ground is recommended. Anti-dust carpets are also required.

Minimise electrostatic area in the clean room : anti-static coating is recommended on the ground. A Mass braid is required around the room.

Storage of slats after assembly : for the first slats produced, there could be about 2 years of storage, before the assembly in CERN. We propose to store each slat in clean and controlled atmosphere.

Lights : movable lights are very useful to see wires on chambers, in addition to the traditional lights in ceiling (these latest lights seem to be not sufficient).

The second part of the document is dedicated to the description of the future assembly rooms for each institute.

4.6.2 Selection criteria of slat's components

All the slat's components have to follow the requirements: some of them are mentionned in 4.1. Each laboratory in charge of the production of a component must assured its quality, control and test.

4.6.3 Steps of the construction procedure

The steps of the construction procedure and the first tests (gas, HV) are written in the document " Slat Integration: Operator's Manual", presented in Annex.

4.6.4 Required tests and checks

In addition to the first tests of gas and HV cited above, we plan a complete readout and relative gain measurements, probably with a source. The exact test for the qualification of a slat is not yet defined in detail.

4.7 Database (item 14)

In order to follow the component production and to store the relevant parameters for each component entering the station 3 4 5 composition, we have added a dedicated section in the ALICE production database developped by the Varsaw ALICE database group.

For the moment few components are entered in the central ALICE database (sandwich panels, spacers, etc...) for which we are defining the parameters to store. The different parameters to define for each component will result from the way to define the quality of the object. This work is under progress. For the sandwich panels for instance we have chosen to store the whole result of the planeity measurement. For each components, its quality, its location, its history are also stored in this database.

A satellite database has also been created in Nantes, with the application to register the defined components. This work will be extended to the other production laboratories.

5 LV segmentation (item 3)

During the PRR of Stations 3-4-5 in Dec. 2001, suggestions about the way of doing the LV segmentation have been made to the Tracking group. Three different ways of segmentation have been studied and discussed between the institutes involved in the Tracking System. The results are presented below with our conclusions.

The main question was : in case of LV Supply breakdown, how many electronic channels will be lost and consequently, can we tolerate such a loss in the Tracking System for the Upsilon mass reconstruction ?

- **Proposition #1** : as the LV Supplies and LV cables have been designed for a maximal current of 25 A, the first proposition, already presented in the PRR document in November 2001, consists of a LV segmentation well adapted to this value. This segmentation leads to a reasonable number of LV Supplies for each Station. **ST3 : 16 LV Supplies ; ST4 : 24 LV Supplies ; ST5 : 24 LV Supplies. In total, we get 64 LV Supplies of 25 A.**

- **Proposition #2** : each slat is supplied individually. This solution leads to a large number of LV Supplies and cables. This maximal solution is not anymore well adapted to the maximum current value. In this case, the maximum current is 14.3 A. **ST3 : 36 LV Supplies ; ST4 : 52 LV Supplies ; ST5 : 52 LV Supplies. In total, we get 140 LV Supplies of 25 A .**

- **Proposition #3** : this proposition is an intermediate solution between proposition #1 and proposition #2. In this case, **ST3 : 20 LV Supplies ; ST4 : 28 LV Supplies ; ST5 : 28 LV Supplies. In total, we get 76 LV Supplies of 25 A.**

- In Tables **??**, **??** and **??**, a comparison between the three propositions is given for each Station. Loss of electronic channels is shown in the last column.

In order to make a correct comparison between the previous propositions, we have to remind how the Tracking System works and look at the number of Υ lost in case of breakdown of one LV supply.

* The Tracking System does not require all the planes to get a track . For example, in Station 3 : 1 plane out of 2 is necessary to get a track ; in Stations 4 and 5 : 3 planes out of 4 are necessary. Even with the maximum loss in Station 3 with Proposition #1 (7.4 %), inefficiency of Station 3 could be 7.4%$\times$4% = 0.29% (Stations have an efficiency of ~ 96%).

Number of Υ hits lost ??

- The Tracking System does not require all the planes to get a track . For example, in Station 3 : 1 plane out of 2 is necessary to get a track ; in Stations 4 and 5 : 3 planes out of 4 are necessary.
  If we consider that one LV supply is not working, the maximum of channels lost is 7.4% (Station 3 with Proposition #1). This corresponds to a percentage of muons from Υ lost in one chamber of Station 3 of 40% (we consider here that we loose one Υ when we loose one muon). To completly loose this muon as a track, the second chamber of Station 3 must be inefficient. This

Station 3 - Chamber 6 Total number of electronic channels for a half chamber = 39936

Proposition 1 : number of LV Supplies is small (PRR Nov. 2001)

Group nb	Nb channels in the group	Nb of slats in the group	Loss of channels (%) in ST3
1	10880	3	6,8
2	11840	2	7,4
3	6336	1	3,9
4	10880	3	6,8

Proposition 2 : one LV Supply per slat : number of LV Supplies is maximum

Group nb	Nb channels in the group	Nb of slats in the group	Loss of channels (%) in ST3
1	2176	1	1.3
2	3264	1	2.0
3	5440	1	3.4
4	6336	1	3.9
5	5504	1	3.4
6	6336	1	3.9
7	5440	1	3.4
8	3264	1	2.0
9	2176	1	1.3

Proposition 3 : intermediate solution between prop.#1 and prop.#2

Group nb	Nb channels in the group	Nb of slats in the group	Loss of channels (%) in ST3
1	10880	3	6.8
2	6636	1	3.9
3	5504	1	3.4
4	6636	1	3.9
5	10880	3	6.8

Table 5.1: Comparison of loss of electronics channels per group of LV Supply, for the three propositions of segmentation.

Station 4 - Chamber 7/8 Total number of electronic channels for a half chamber = 55168

Proposition 1 : number of LV Supplies is small (PRR Nov. 2001)

Group nb	Nb channels in the group	Nb of slats in the group	Loss of channels (%) in ST4
1	10624	4	4.8
2	7104	1	3.2
3	12608	2	5.7
4	7104	1	3.2
5	7104	1	3.2
6	10624	4	4.8

Proposition 2 : one LV Supply per slat : number of LV Supplies is maximum

Group nb	Nb channels in the group	Nb of slats in the group	Loss of channels (%) in ST4
1	1152	1	0.5
2	1728	1	0.8
3	3328	1	1.5
4	4416	1	2.0
5	7104	1	3.2
6	7104	1	3.2
7	5504	1	2.5
8	7104	1	3.2
9	7104	1	3.2
10	4416	1	2.0
11	3328	1	1.5
12	1728	1	0.8
13	1152	1	0.5

Proposition 3 : intermediate solution between prop.#1 and prop.#2

Group nb	Nb channels in the group	Nb of slats in the group	Loss of channels (%) in ST4
1	10624	4	4.8
2	7104	1	3.2
3	7104	1	3.2
4	5504	1	2.5
5	7104	1	3.2
6	7104	1	3.2
7	10624	4	4.8

Table 5.2: Comparison of loss of electronics channels per group of LV Supply, for the three propositions of segmentation.

Station 5 - Chamber 9/10 Total number of electronic channels for a half chamber = 60928

Proposition 1 : number of LV Supplies is small (PRR Nov. 2001)

Group nb	Nb channels in the group	Nb of slats in the group	Loss of channels (%) in ST5
1	7936	3	3.2
2	12672	2	5.2
3	12608	2	5.2
4	7104	1	2.9
5	12672	2	5.2
6	7936	3	3.2

Proposition 2 : one LV Supply per slat : number of LV Supplies is maximum

Group nb	Nb channels in the group	Nb of slats in the group	Loss of channels (%) in ST5
1	1728	1	0.7
2	2304	1	1.0
3	3904	1	1.6
4	4992	1	2.0
5	7680	1	3.1
6	7104	1	2.9
7	5504	1	2.2
8	7104	1	2.9
9	7680	1	3.1
10	4992	1	2.0
11	3904	1	1.6
12	2304	1	1.0
13	1728	1	0.7

Proposition 3 : intermediate solution between prop.#1 and prop.#2

Group nb	Nb channels in the group	Nb of slats in the group	Loss of channels (%) in ST5
1	12928	4	5.3
2	7680	1	3.1
3	7104	1	2.9
4	5504	1	2.2
5	7104	1	2.9
6	7680	1	3.1
7	12928	4	5.3

Table 5.3: Comparison of loss of electronics channels per group of LV Supply, fot the three propositions of segmentation.

happens maximum 8% of the time (see chapter 2, 92% efficiency at 3 σ; this is pessimistic because we consider that we loose completly a hit in 8% of the time). As a consequence, the percentage of muon tracks and therefore ϒ losses is 3.2%.

- Proposition #3 (maximum percentage of channels lost is 6.8 %) gives a maximum of 20% of muons from ϒ lost in one chamber, reducing by a factor of 2 the percentage of ϒ s' lost to 1.6%, which seems reasonable. The number of LV supplies is then increase by 12 units compared to proposition #1.

Conclusion : Institutes involved in Stations 3-4-5 are in favour of **proposition #3**, with 76 LV Supplies of 25 A**.**

6 Flatness and tolerances of the panel support, fixation of slats (item 15+16)

We remind first what was at the PRR period, the slats supports and also the slats fixation, which were already not constrained (this point had not been presented clearly).

Then we present the improvements mainly coming from a new approach of the slats positioning; these improvements will help in feasibility and in price reduction.

6.1 Slats supports with the slat positioning system (before PRR Nov. 2001)

6.1.1 Conception of the support and fixations of slat principle (before PRR Nov. 2001)

- Flatness of the support :

At the end of 1999, the recess, imposed for the tracking chambers, had to be as small as possible, because it was located on the porter structure of the beam shield. In the same time, the Stations had to be as compact as possible, for physics reasons. The proposed slats supports had then to be very thin (thickness of 15 mm) and should have a flatness tolerance as small as possible, because of the reduced room at the level of the recess.

In this context, in order to give a right number for the flatness, few visits have been organized in french companies. We learnt that a 2 mm flatness seemed to be feasible for the bigger support (5.70 m height), but this flatness was already hard to achieve. If we consider a flatness superior to 2 mm, then there will be a risk, in

some places, of quasi-contact between electronics of slats and panel support. This could lead to a bad cooling of the electronics.

- Material :

The panel has to support the weight of all slats with electronics and cables, presenting the smallest possible deformation ($\delta_{maxi} < 1$ mm for a total weight estimated to 230 kg for the Station 5). Several calculations have shown that carbon fibre is an appropriate material to obey to this constraint. Moreover, we need a support which has the smallest deformation as possible by thermal dilatation. Carbon fibre presents this advantage with an excellent thermal behaviour with a small thermal dilatation coefficient : $\sim 5 \times 10^{-6}/^{\circ}\mathrm{C}$ for carbon fibre with resin (the maximal deformation is then equal to 600 microns for a δT of 20 $^{\circ}$C and for a length of 6 m).

- Positioning and fixations of slats on the support :

The knowledge of the pads coordinates, which are on the Printed Circuit Boards, is necessary for physics; this is done in two steps :

1. During the slat assembly, the position of the pads is well known and given by two calibrated holes at each extremity of the slat. The positioning of the slats is made with the help of inserts, placed in the panel support. Of course, these inserts are out of the detection area.

2. Two centering calibrated axis, adjustable and drilled for surveyors target, are foreseen to receive each slat. During the mounting of the slat on its support, the reference is always the two centering axis.

- Positioning in z (beam direction) :

The slat comes in contact with the support on four pins. The slat is maintained on these pins by screws and spring disks (these latest avoid any constraint on the slat). Figure 6.1 illustrates the principle of the slat fixation on the panel support.

The four pins of one slat are within a plane of 0.5 mm flatness and all the pins, in the whole support (5.70 m maximum), are within a plane of 2 mm thickness. This area of 0.5 mm of flatness on 300 mm in height guarantees an angle in z equal to 0,095° at maximum. This maximum angle is considered as negligible and consequently, there is no adjustment foreseen in z for the slats.

- Positioning in x and y :

The right position in x and y is assured by the two adjustable centering axis (adjustment of $\pm$ 1,5 mm) on the panel support. Each slat is mounted on these two axis. Both axis are then overtightened on the support.

The position in x of the slat is assured by the adjustment of the first centering axis, the second one is free in an oblong groove. The position in y is assured by the adjustment of the two centering axis.

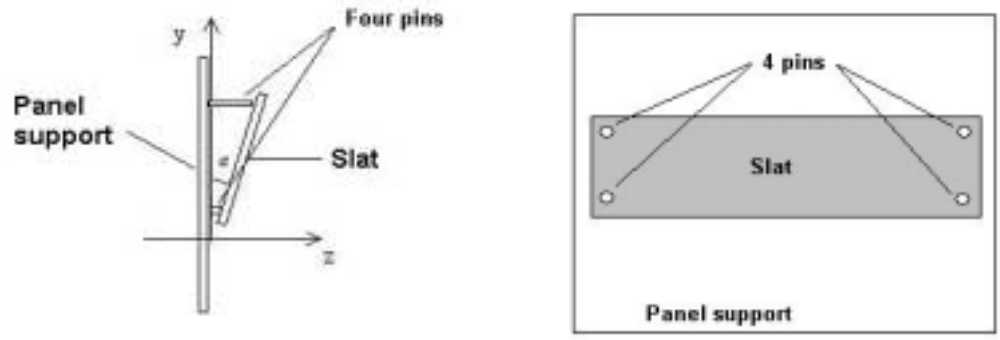

Figure 6.1: Left : representation of the positioning of the slat in z on four pins with its maximum angle equal to 0.095° (not to scale). Right : assembly of one slat on its panel support.

6.1.2 Slat positioning system (before PRR Nov. 2001)

Physics needs to know the positions of all the pads and thus of all slats, with a precision less than 100 μm in x, y and less than 200 μm in z. The control of these positions can be done by photogrammetry technique, which allows to reach the required precisions.
Moreover, we thought that it could be useful to apply some angular corrections, for each slat individually, and a special mechanical device had been designed and realized to allow very small adjustments of each slat : up to 2 mm with steps of 10 μm. This positioning device had been tested and validated by photogrammetry technique. The principle of the tests are explained below.

The Survey targets are installed on different places on the panel support and on slats (in centering axis) and the positions are given by a set of photographs of these targets. The slat is mounted to its theoretical position as well as possible. A first collection of photographs is done. In function of the results obtained, the slat is mechanically positioned again in x and y with the platen system. Figure 6.2 shows the platen used for the slat adjustment in x and y. In order to move the slat, the two targets, which are in the centering axis, are removed. The head of the device, connected to the platen, is introduced and allows to adjust the slat in x and y. The position z is given by the assembly and is well sufficient for the physics.

The slats adjustment steps are :

1. All slats are mounted as well as possible, in the middle of their play of adjustment.

2. Slats are fixed and a first set of photographs is taken to locate the positions of the targets in comparison with reference points placed on the panel support.

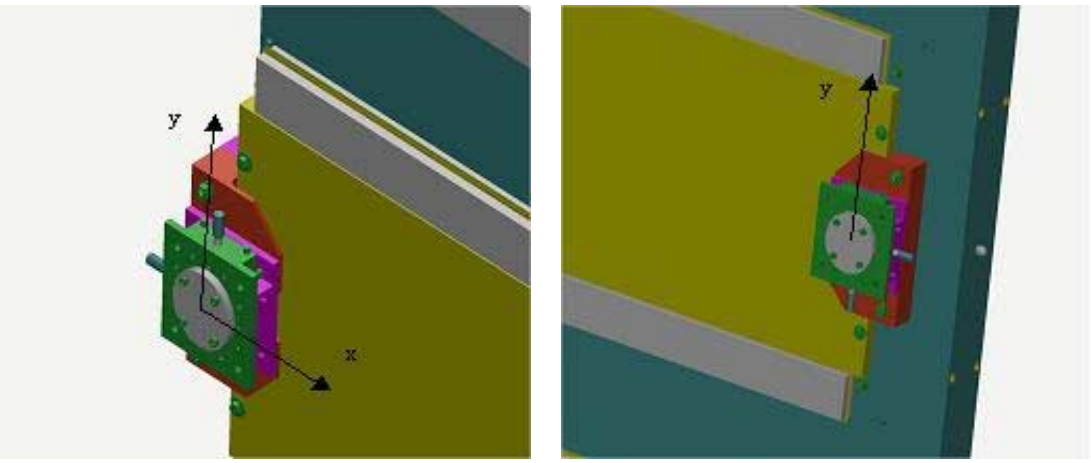

Figure 6.2: Left : adjustment of the first centering axis in x and y (beam shield side). Right : adjustment of the second centering axis in y only (external side).

3. Adjustment of the inner part: the positioning system is placed on the first centering axis (closed to the beam-shield) and we can tune in x and y, according to the results of the photogrammetry. The second axis, mounted in an oblong groove and not jammed, can follow the displacement in x of the first axis.

4. The first point is jammed in position, once adjusted.

5. The positioning system is placed on the second centering axis (outer part), and the oblong groove is not jammed. The adjustment of the second point in y can be performed. The groove is then jammed. We try to adjust x and y in a range of $\pm$ 1,5 mm at maximum.

6. We check the right position of the slats by a last set of photographs.

Remark : In order to test this mechanical device, Saclay has built an Aluminum mock up of the central part of Station 5 with its 5 slats. This system has been validated with a campaign of measurements done by photogrammetry. All results are reported in a Preprint submitted to ALICE Note in January 2003.

6.2 Slats supports (after PRR ~ March 2002)

6.2.1 Conception of the support (after PRR ~ March 2002)

The flatness of the support being the most difficult constraint for companies, many specialists have been visited again in order to determine with them an easier accessible flatness for a lower price. We learnt that a flatness of 2 mm, considered at the beginning, is very hard to achieve and is at the limit of manufacturing for some companies.

Taking into account these important informations on the way of realization,

physicists ask to increase the recess and moreover the distance between electronics and supports has been increased too. The recess is now made of lead modules for Stations 4 and 5 and it is now possible to increase its length relatively easily. Today, this modification on the recess length leads us to consider reasonably a new flatness of 10 mm. This value is easily achievable by many facturers.

The main characteristics of the support stay the same as in the previous conception :

- Amount of matter must be as small as possible : X/Xo < 0.3 %.

- Panels have to support a total weight of 230 kg for the bigger Station (weight the panel itself, weigth of electronics, slats and cables).

- The weight of the panel, with its internal bars, must be as light as possible.

- Panels thermal dilatation must be as small as possible ($\alpha_l < 5 \times 10^{-6}/^{\circ}\mathrm{C}$).

- Panel must be as rigid as possible (E/ ρ > > 100 MPa/kg/m^3).

- Panel Flatness does not exceed 10 mm.

- Position of all slats must be known with a precision less than 100 μm in the x and y directions and less than 200 μm in z.

- A misworking slat must be replaced by a new one without doing new measurements of its position.

In order to respect as well as possible the mechanical deformation and thermal dilatation constraints, many calculations have shown the following results :

1. Carbon fibre is the most appropriate material.

2. The use of sandwich panels, with a honeycomb structure, covered by two skins in carbon fibre, is the best choice, especially because of its small deformation (the maximal deformation stays below 1 mm for the bigger panel loaded with 230 kg). Dimensions of the bigger panel are shown in figure **??** for Station 5 : 5700 mm x 2600 mm x 15 mm.

6.2.2 New fixations of slats on the support

During the assembly of each slat, the position of pads is known very precisely in relation to the two calibrated axis A and B. Each slat will be fixed by these two points A and B on the support.

Figure 6.4 illustrates the principle of the new slat fixation. At point A, the slat is tightened, bearing on a plane straight edge, by the calibrated axis (in red on the figure 6.4). This plane straight edge offers a good surface of contact to the slat.

At point B, the slat is also tightened by the second calibrated axis, but through a convex disk which avoid any torsion related to the rigid point A. Two screwed rods will be beared on the panels, without constraint for the slat.

The geometrical position of assembly is given by the machining tolerance of the inter-axis of the fixation holes. We asked for a precision of ± 0.5 mm).

Parallelism between each slat could be tuned, if necessary, in Point A, including wedges with variable thickness under the plane straight edge. By this way, some

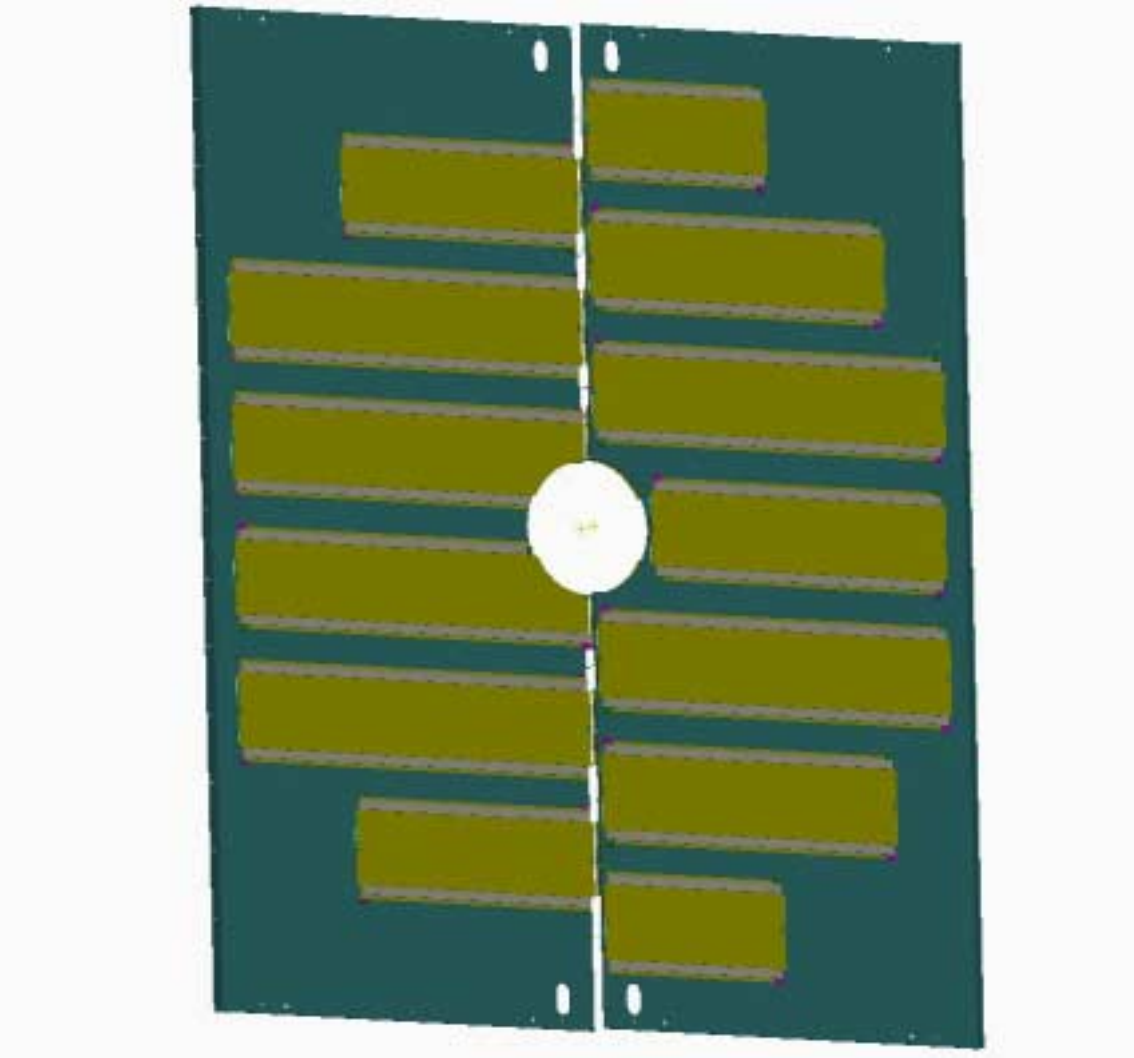

Figure 6.3: Chamber 10 of Station 5, composed of 2 panels support with slats of detection. Dimensions of each support of Station 5 are : 5700 mm x 2600 mm x 15 mm. Four big holes (top and bottom), for example, are used for the passage of the vertical lines of the Geometry Monitoring System.

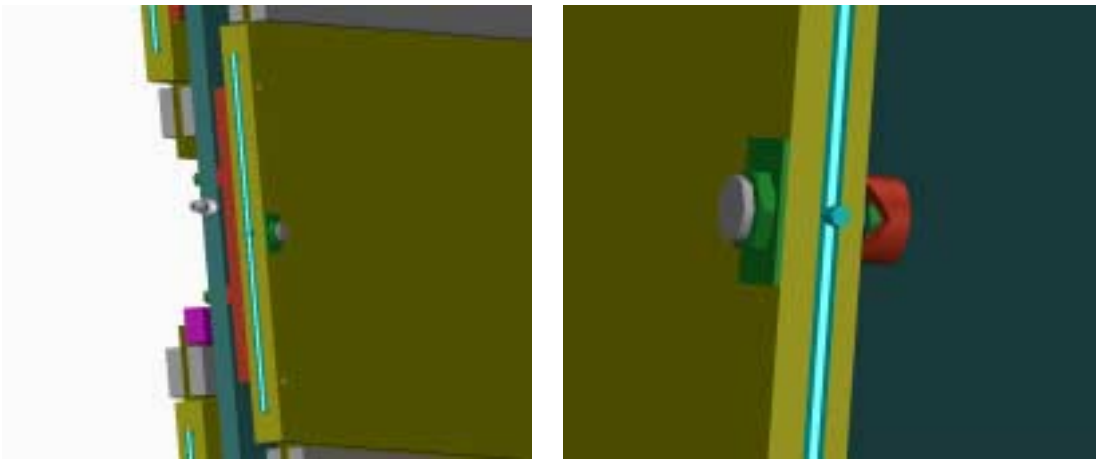

Figure 6.4: Principle of the new fixation of slat. Left : point A fixation, in the internal side of the chamber, closed to the beam pipe. Right : point B fixation, in the external side of the chamber.

possible default in the flatness of the support can be corrected.

6.2.3 Position of slats

The measurement of position in x, y and z of all slats will be realized by photogrammetry.

Some tests, done in CEA Saclay in February 2002, on a mock up of Station 5 at scale 1, have shown that the precision of measurements obtained by photogrammetry is less than 100 μm in the three directions. These results, sufficient for physics, have allowed to suppress the mechanical positionning system described in 6.1 (presented in PRR document in November 2001).

In Points A and B, a calibrated hole in each axis is foreseen to receive plane targets. Those targets, in addition to the non-coded targets (ruban), will give all positions of slats in x, y and z on each face of the support.

Some other spherical targets will be installed on the panel edges, in calibrated holes. These lattest targets allow to establish the geometrical link between position of slats on one panel's face, compared to slats of the other face (see 6.5).

7 Alignment monitoring (item 17)

We remind that the Tracking group is not in charge of the Geometry Monitoring System. We assure only the integration aspects of the system : passage of the lines and room for the Rasnik elements on panels. The design of Rasnik elements is not

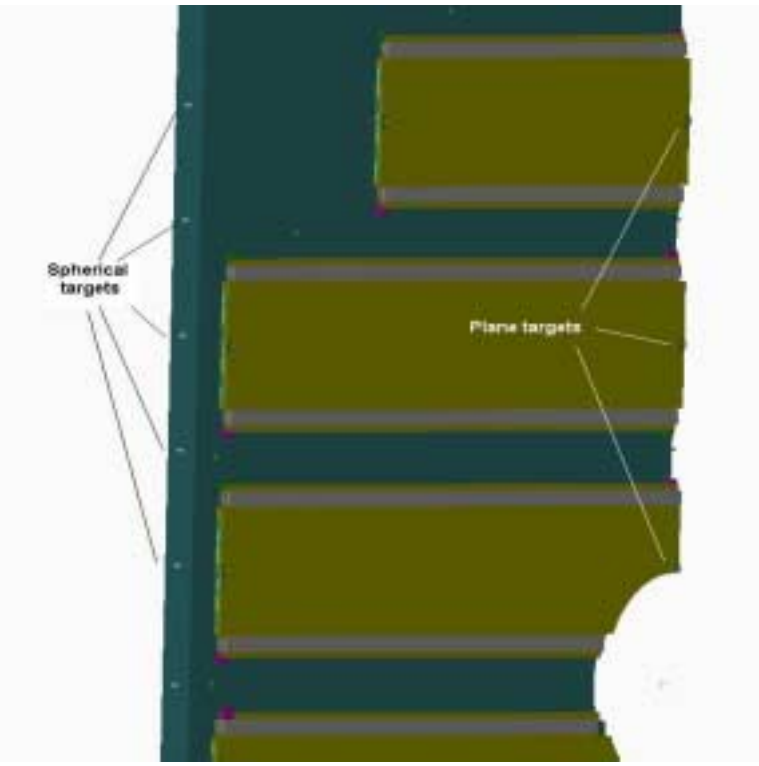

Figure 6.5: Position of plane and spherical surveyor's targets.

completly frozen today, as IPN Lyon is still studying the system.

Figures 7.1 and 7.2 illustrate the integration of all lines of the GMS in Stations 3-4-5, in October 2002. Large holes in panel supports are foreseen for the lines passage. Integration aspects on panel supports are very important and few meetings have been organized during the year 2002 in order to converge to the solution proposed today (on figure 7.2). The present solution suits well to Saclay and IPNL. It remains small details on Rasnik boxes location to be studied by IPNL, but it will not change the design of the present lines.

In any case, the order of the panels market must be launched beginning 2003 and every supports have to be then final.

8 Cooling (item 18)

A new study of the cooling of stations 3, 4 and 5 is led at the moment at CEA Saclay. This study has been divided into 3 stages. The first stage is now finished, and the second stage is about to begin.

8.1 Modeling of station 1 mock-up

8.1.1 Aim

The aim of this first stage is to validate our numerical model with experimental results. Indeed, due to the impossibility for CEA Saclay to conduct a real mock-up experiment of the stations 3, 4, 5 cooling, the first simulations performed during the 2000 and 2001 years (with the fluid dynamics software Star-CD®), could never be validated by experimental results. To have a larger trust in our numerical results, it was decided, with IPNO's agreement, to use the experimental results obtained by IPNO for stations 1 and 2, from a full scale experiment. This experiment, which is briefly described later and was led 2 years ago, consists of a mock-up of stations 1 and 2 which is instrumented to simulate the increase of temperature of these stations during functioning.

The approach is the following one :

- modeling, with our software, of the experiment done for stations 1 and 2
- comparison of the results obtained numerically and experimentally
- adjustment and validation of our numerical model.

Then our numerical model will be safely used to study first station 3, which has the most critical thermal conditions, and then stations 4 and 5.

Note that IPNO, which is responsible for the cooling of stations 1 and 2, has already used the experimental results of their mock-up to validate their numerical model built for the study of these stations (model performed with the software

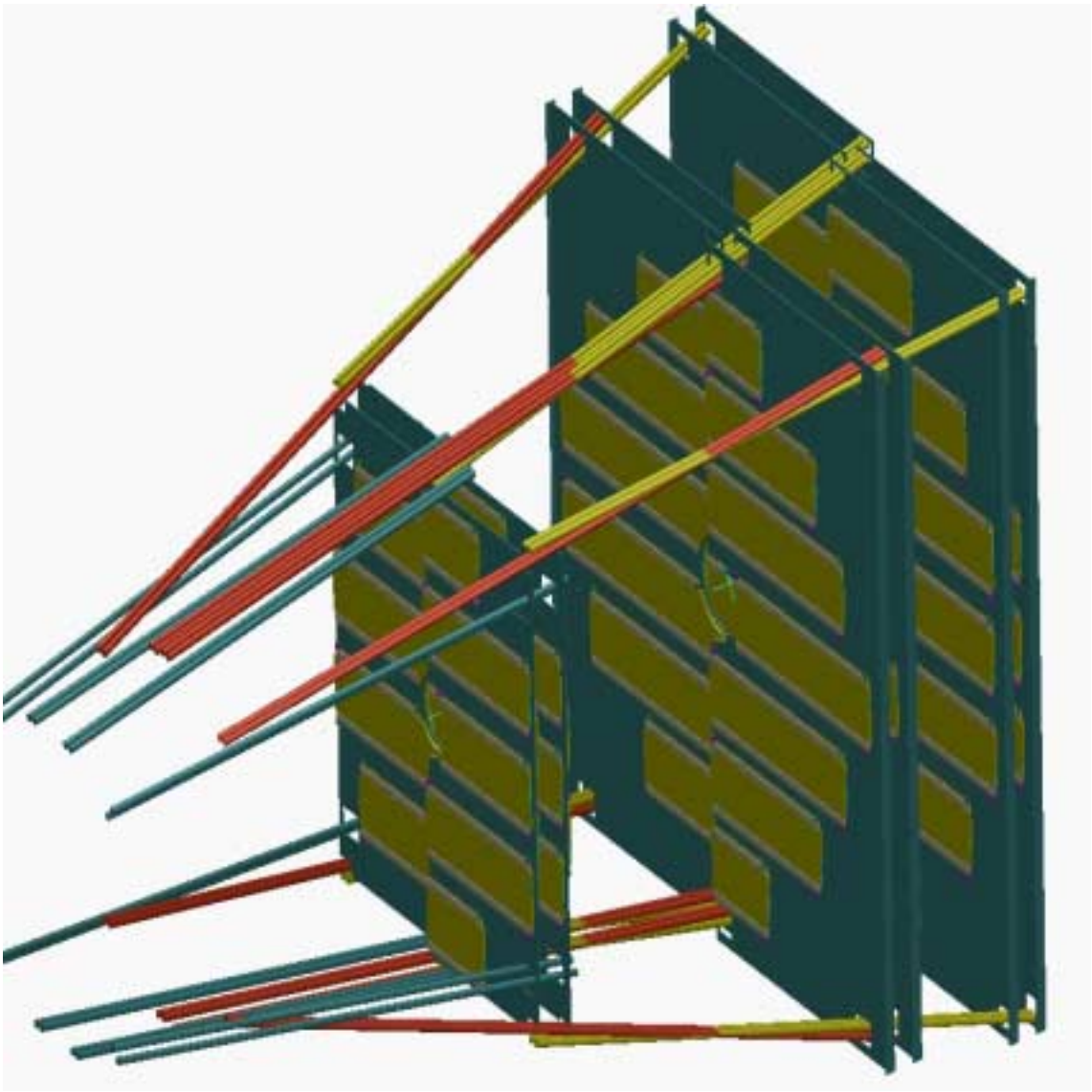

Figure 7.1: Integration of the Geometry Monitoring System. 3D view of the passage of GMS lines through the Stations 3-4-5.

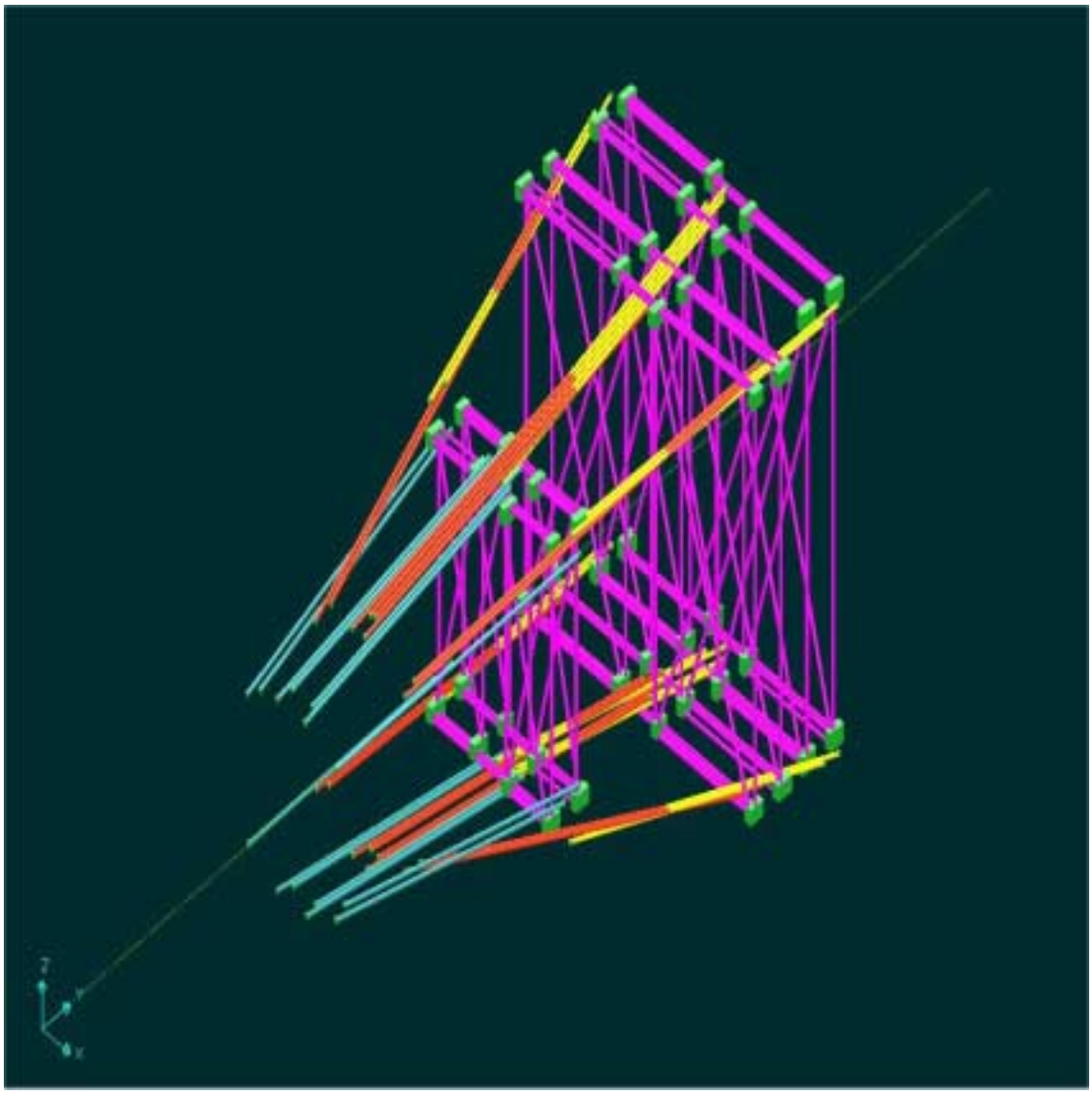

Figure 7.2: Integration of the Geometry Monitoring System. 3D of all Rasnik lines and elements. Horizontal, vertical and crossing lines are necessary to monitor panel supports.

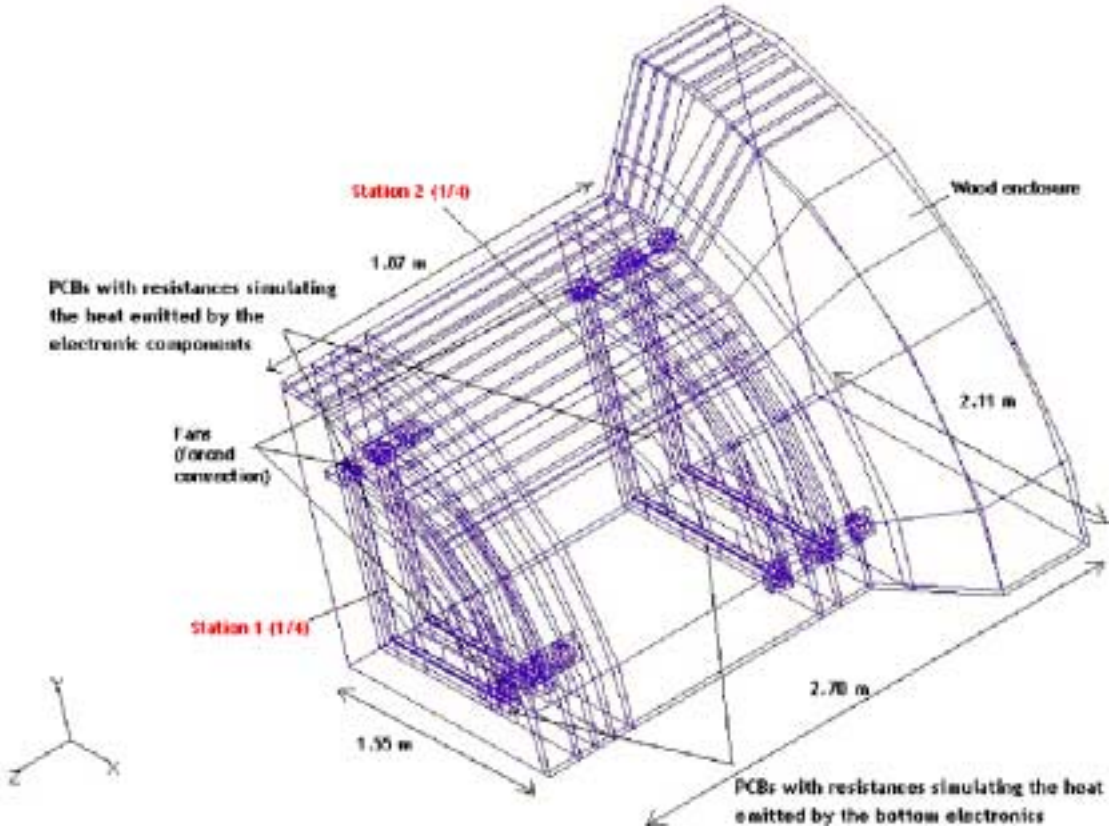

Figure 8.1: Layout of IPNO mock-up

Ideas® from SDRC). Another point to underline is that the simulations of this new study are realized with a new fluid dynamics software, which is CFDesign® from Blue Ridge Numerics.

8.1.2 Description of the mock-up

Only a quarter of stations 1 and 2 has been represented (see figure 8.1).

The real geometrical environment of the stations, that is the Front Absorber Support, is represented by a wood enclosure. Each station is composed of two chambers, each of them is represented by two planes of circular PCBs. The heat emitted by the electronic components of the PCBs is reproduced by resistances fixed on them. To take into account the heat emitted by the electronics of the missing down part of the stations, some additional rectangular PCBs, with resistances emitting heat, have been placed at the base of the stations. There is also a set of copper plates on the ceiling of the housing which are cooled by a coil of cold water (20°C). Two sets of three fans are placed at the top and the bottom of each station ; they are used to improve the cooling of the stations by creating a forced convection of the air around them. Finally, the temperatures are measured through temperature gauges which are located on planes situated at 15 mm of the PCBs planes.

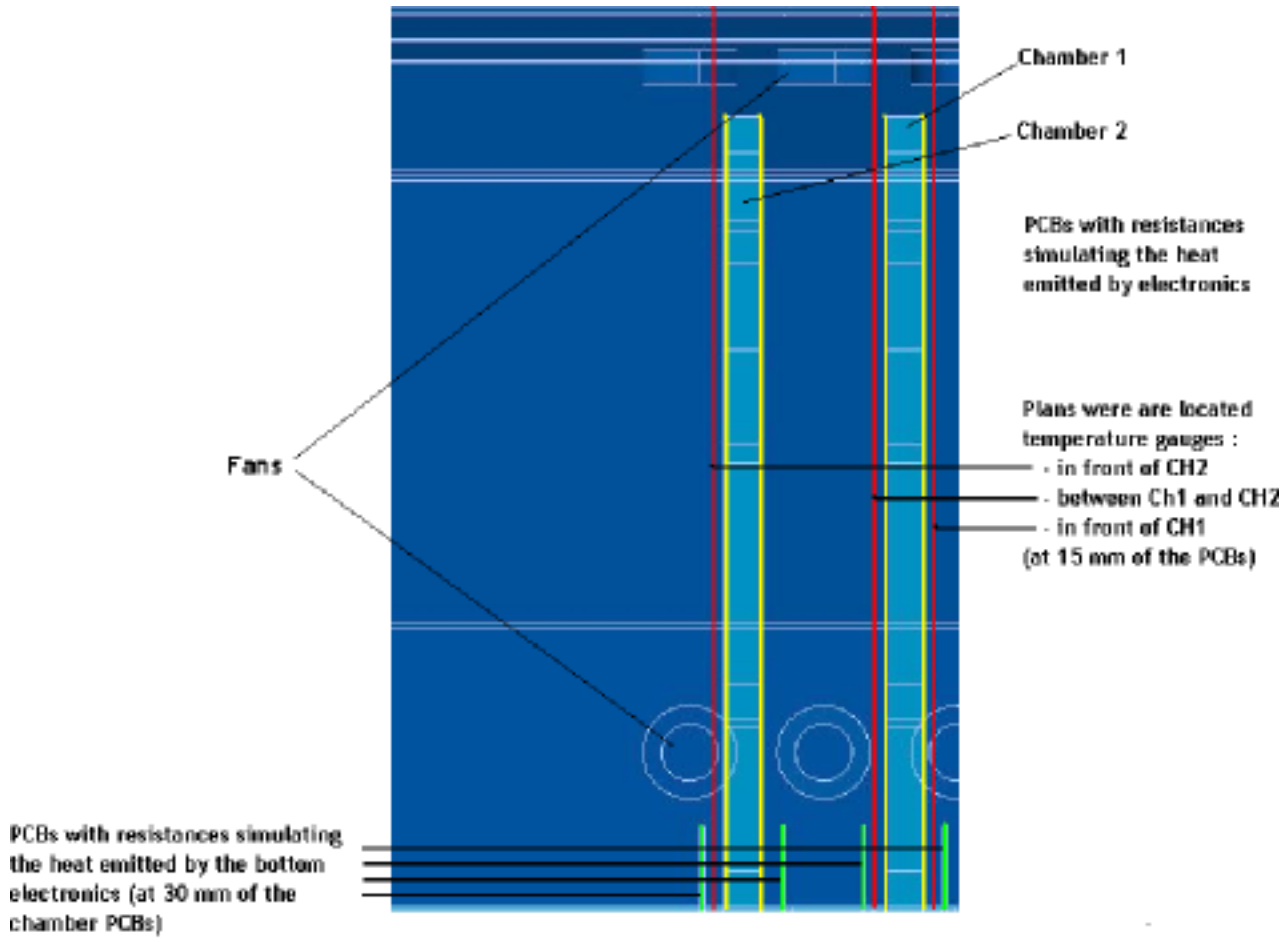

Figure 8.2: Side view of station 1 modeling

To simplify the numerical modeling, only station 1 has been represented. This station is composed of chambers 1 and 2 which emit a total heat of 1145 W (497 W are emitted by the resistances of the circular PCBs, 648 W are emitted by those of the rectangular PCBs).

Figure 8.2 shows station 1 modeling seen by the side, where the planes of temperature gauges are represented in red : there are 6 gauges in the planes in front of chamber 1 and in front of chamber 2, and 16 gauges in the plane between the 2 chambers.

8.1.3 Calculations hypothesis

The modeling which has been built is rather complete, since even the conduction in the solid components (wood enclosure, PCBs in glass epoxy) has been taken into account, as well as the convection between the wood housing and the environmental air (room temperature of 24°C). The resulting model is huge (approximately 260000

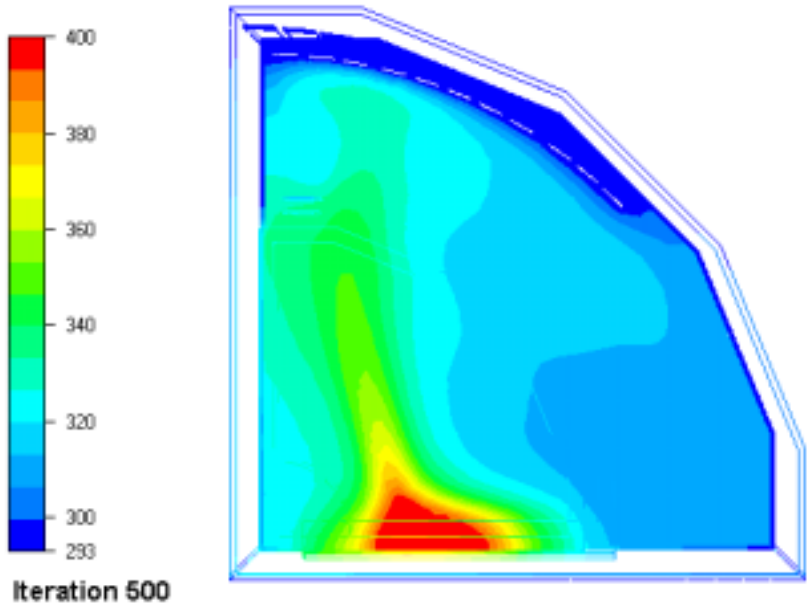

Figure 8.3: Natural convection - Air temperatures (K) in the gauges plane between the 2 chambers of station 1

elements and 56000 nodes), and the time which is necessary for the convergence of one calculation is about 10 to 15 hours. Two types of convection have been studied : first natural convection, then forced convection, obtained with the switching on of the fans. Concerning the turbulence of the air, the model which is applied is the "Eddy viscosity" model.

8.1.4 Results of the calculations

8.1.4.1 Natural convection

As expected, the temperatures obtained are very high, due to the low speed of the air. Figures 8.3 and 8.4 respectively show the temperatures and the speeds of the air in the gauges plane between the 2 chambers of station 1 (hotest one).

Figure 8.5 below gives, for the gauges between the 2 chambers of station 1, the comparison between the measured temperatures obtained by the gauges, and the calculated temperatures provided by the numerical simulations.

The first remark is that temperatures between the 2 chambers of station 1 are roughly contained between 50 and 70°C. Moreover, figure 8.5 shows that the adjustment between measurements and calculations is not very good, mostly for gauge 41 which gives a measured temperature of 68°C, while the calculation gives a value of nearly 120°C. This high difference is certainly due to the uncertainty of the outline of the hot zone at the station bottom (red zone in figure 3), since gauge 41 is

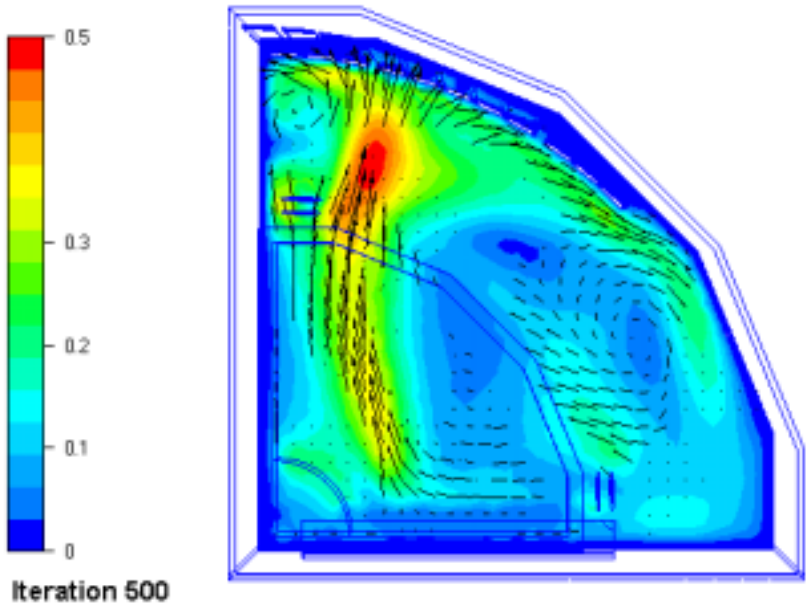

Figure 8.4: Natural convection - Air speeds (ms-1) in the gauges plane between the 2 chambers of station 1

situated in the vicinity of this outline.

Nevertheless, these discrepancies are not so worrying, since natural convection is known as difficult to simulate.

8.1.4.2 Forced convection

The forced convection is obtained by switching on the 6 fans around station 1, each fan blowing an air flow of 85 m^3/h. Figures 8.6 and 8.7 give the resulting temperatures and speeds of the air between the 2 chambers of station 1.

Figure 8.8 below gives, for the gauges between the 2 chambers of station1, the comparison between the measured temperatures obtained by the gauges, and the calculated temperatures provided by the numerical simulations.

The effect of the fans is obvious : the temperature at the gauges are now contained between 40 and 50°C. Besides, the adjustment between measurements and calculations is here very satisfactory. Table 8.1, which gives the values of these measured and calculated temperatures and the differences between these values, shows that the maximal absolute difference is 6°C and the maximal relative difference is 15%.

This good adjustment allows to conclude that the modeling of forced convection can be considered as reliable. As the cooling of stations 3, 4, 5 will necessarily need a forced convection of the air, we can reasonably estimate that our numerical model is validated.

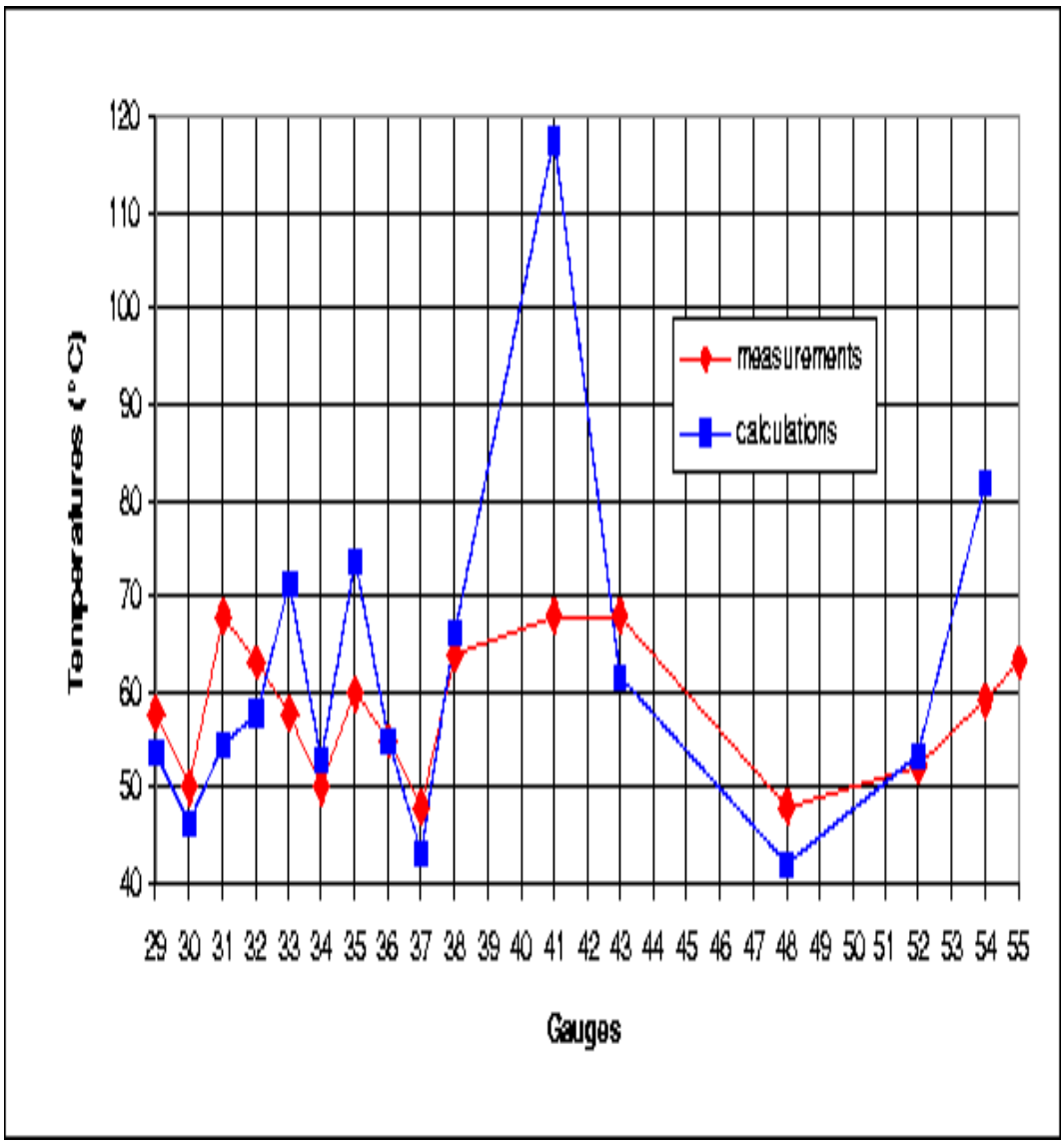

Figure 8.5: Natural convection - Comparison of calculated and measured temperatures between the 2 chambers of station 1

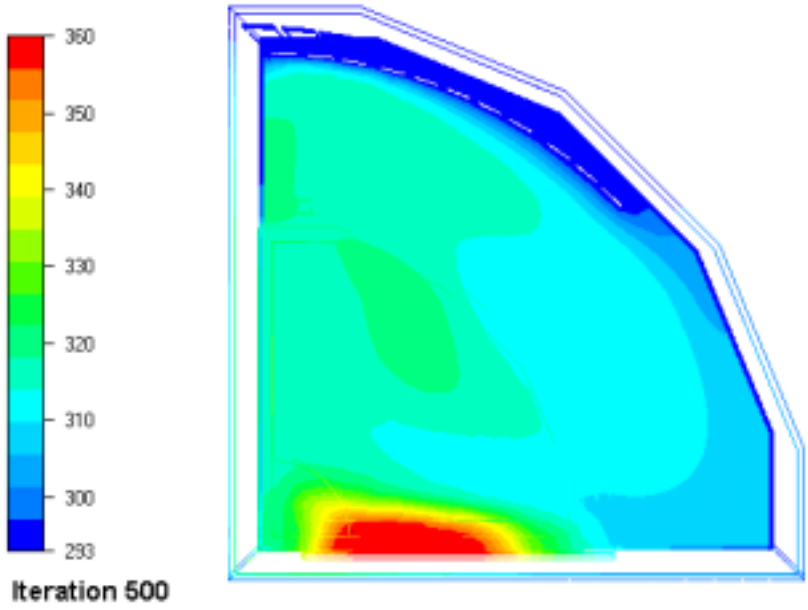

Figure 8.6: Forced convection - Air temperatures (K) in the gauges plane between the 2 chambers of station 1

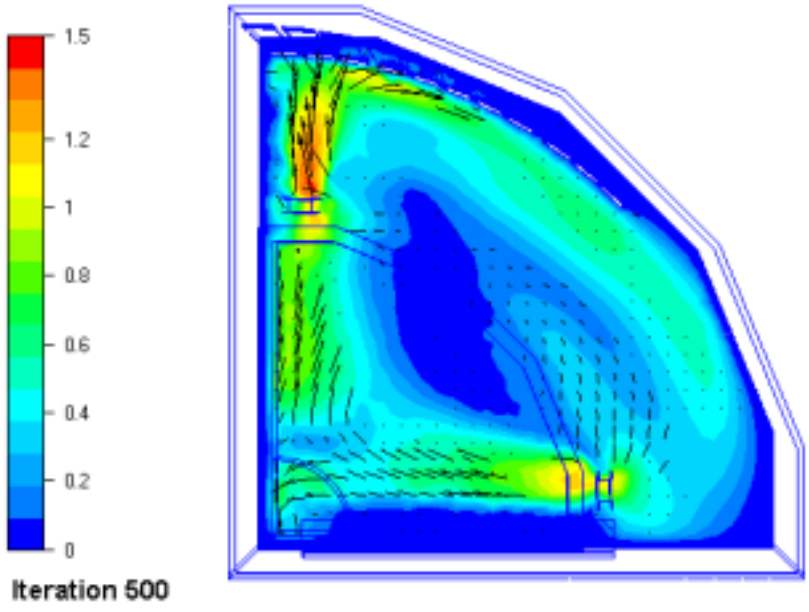

Figure 8.7: Forced convection - Air speeds (ms-1) in the gauges plane between the 2 chambers of station 1

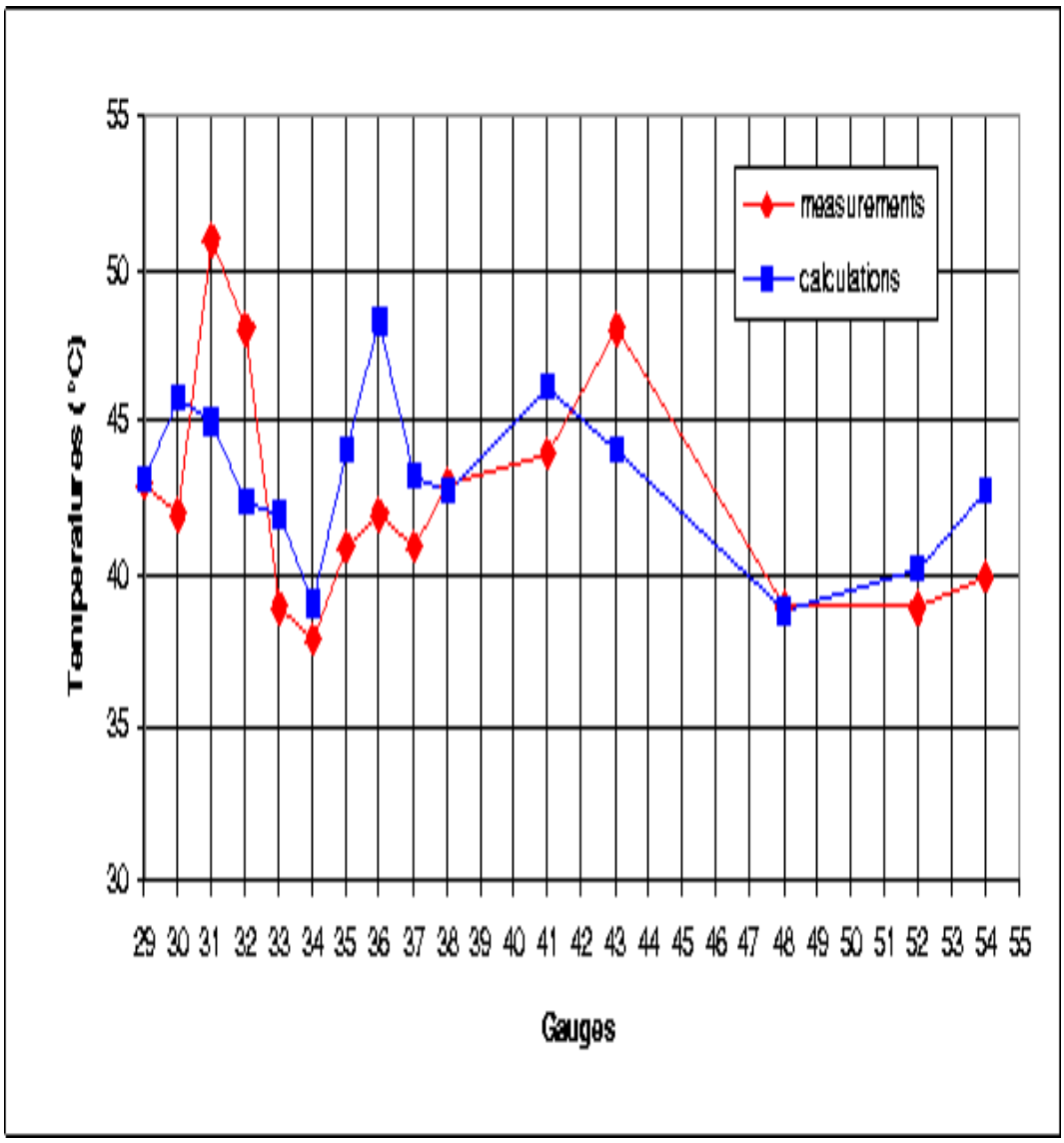

Figure 8.8: Forced convection - Comparison of calculated and measured temperatures between the 2 chambers of station 1

	Measured temperatures (°C)	Calculated temperatures (°C)	Absolute temp. difference (°C)	Relative temp. difference (%)
29	43	43.1	-0.1	-0.2
30	42	45.8	-3.8	-9.0
31	51	45.0	6.0	11.8
32	48	42.4	5.6	11.7
33	39	42.0	-3.0	-7.7
34	38	39.1	-1.1	-2.9
35	41	44.1	-3.1	-7.6
36	42	48.3	-6.3	-15.0
37	41	43.2	-2.2	-5.4
38	43	42.8	0.2	0.5
41	44	46.1	-2.1	-4.8
43	48	44.2	3.8	7.9
48	48	38.8	0.2	0.5
52	52	40.2	-1.2	-3.1
54	59	42.8		-7.0

Table 8.1: Forced convection - Comparison of calculated and measured temperatures between the 2 chambers of station 1

8.2 Modeling of station 3

Now that the model has been validated, the second step, modeling of station 3, is ready to begin.

The thermal situation of station 3 is critical since :

- this station is situated inside the dipole magnet, which forms a box around it and prevents heat from being evacuated

- the dipole coils emit a certain quantity of heat, which adds to the heat emitted by electronics components of slats.

It is first foreseen to perform calculations which simulate three inlets of cold air at the base of the station : two big inlets on the two sides, and a small inlet at the middle (the size of the inlet is here limited by the existence of a support for the coils). If these inlets are not sufficient to decrease the temperature around the station, the injection of cold air will also be done by the top of the station. The warm air will be evacuated either directly in the cavern if its temperature is not too high. The calculations will first be performed by sending cold air with a small speed (about 1 m/s), to impose a slow air flow around the station and to avoid high turbulence and vibrations of slats and their supports. If the results show that the air speed is not sufficient to permit an uniform cooling of the station, we will be obliged to impose a higher air speed at the inlets. The effect of this turbulent air on the possible movements of the slats and their support will then have to be assessed.

8.3 Modeling of stations 4 and 5

The situation of stations 4 and 5 is less critical since the circulation of air around them is not hindered by obstacles. We are going to model their cooling by extractions of air situated at their top. Inlet of cold air at the base of the stations will only be introduced if its appears necessary. To canalize the air flow along the slats planes, we will maybe have to add some curtains of mylar between the dipole and station 4, and between station 5 and the muon filter.

8.4 Temperature measurements on the electronics

This section takes up again the Orsay Note on the temperature measurements on the electronic chips and the PCBs.

Set-up

Measurements have been done on a part of a slat equipped with 7 MANU345 (with Gassiplex 0.7) on both bending and non-bending planes (Fig. 8.9). Temperatures were read by a probe with CTN calibrated resistor (Thermistor Temperature Probe HPE2308A) with an intrinsic precision on $\pm 0.2\ ^{\circ}$C. The thermal contact was insured by a colloid. The final precision was estimated to $\pm 1^{\circ}$C. The same probe was used to measure the ambiant temperature (~22° C) and the one of the components.

Thermalisation time

To check that the thermal equilibrium has been reeched, the temperatrure was measured as a function of time from the voltage switch on (Fig. 8.10).

Chips consumption:

The low voltage supplies for the MANU345 was +2.75 V, -2.75 V and +3.3 V.

Measured currents were : 0.8A for +3.3 V, 1.4A for +2.75 V and 1.65A for -2.75 V.

The total consumption was 12.3mW/channel (9.4 mW for Gassiplex and 2.9 mW for digital part (MARC,ADC,...). This power has been measured during the read-out but with a low rate ~ 1 Hz.

Measured temperatures on chips:

Measurements were done on 3 Gassiplex 0.7-3 μm: the temperature difference between **Gassiplex package** and ambiant temperature is :

$$\Delta T = 15.5\ ^{\circ}C$$

This corresponds to a difference of temperature on the **silicon chip** compared to ambiant temperature of :

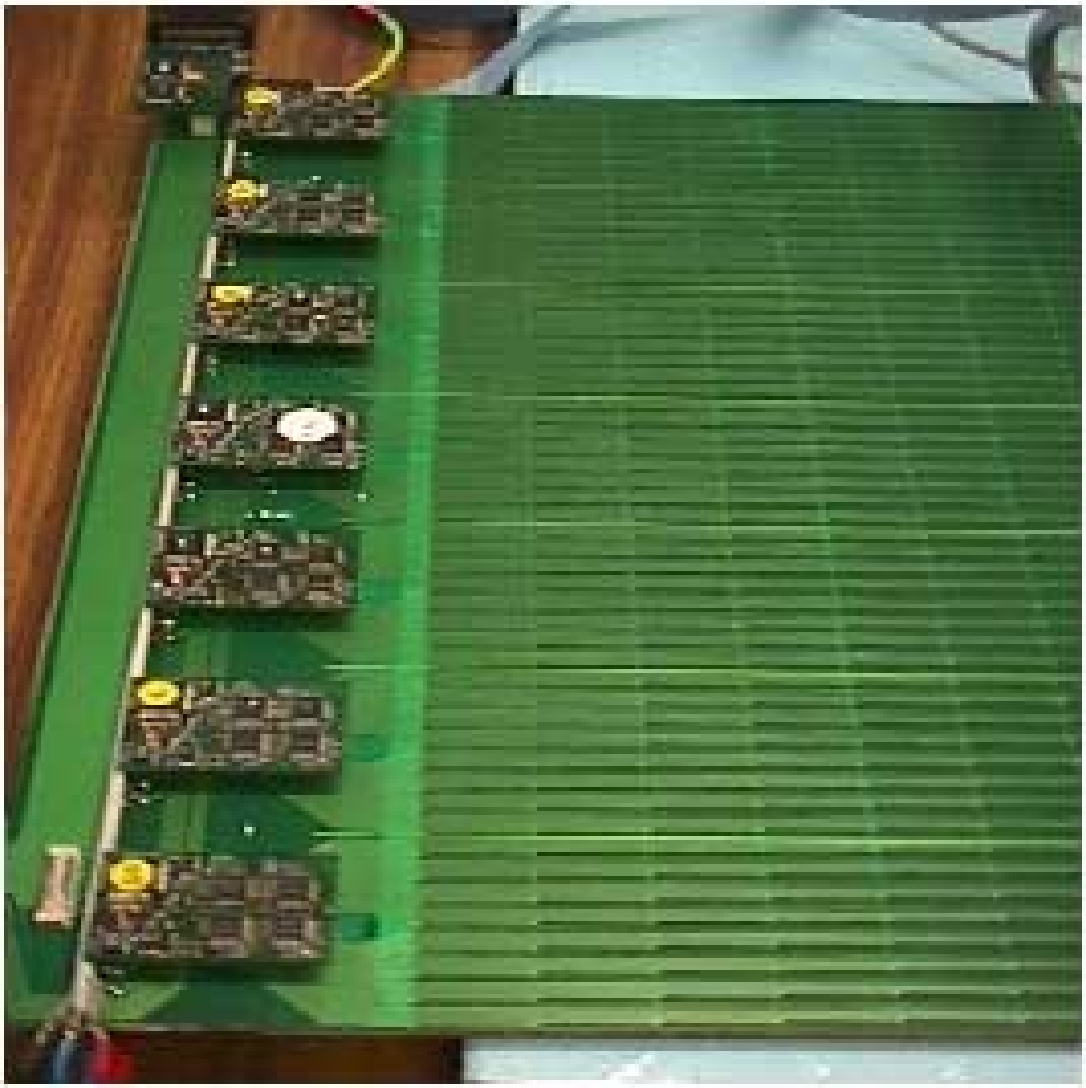

Figure 8.9: View of the PCBS used for measurements

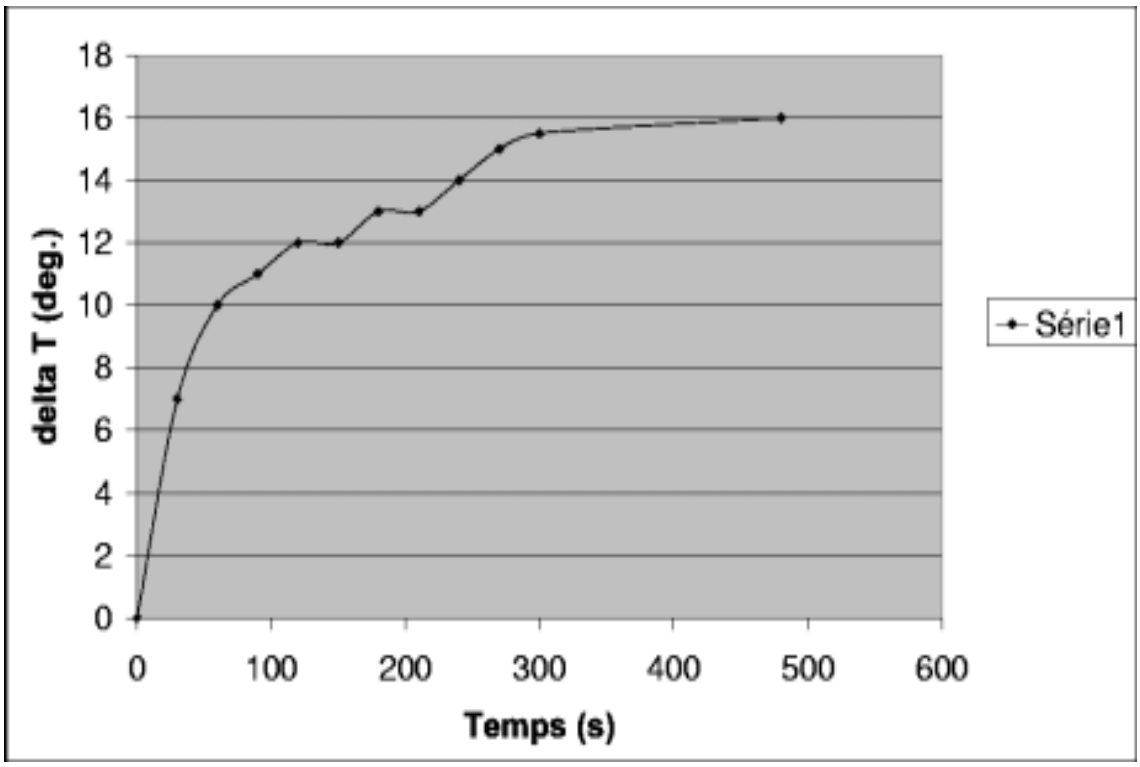

Figure 8.10: Variation of GASSIPLEX temperature as a function of time from the voltage switch on.

$$\Delta T = 26.2\ ^{\circ}C$$

Measurements made on 2 MARC give (compared to ambiant air):

$$\Delta T = 9\ ^{\circ}C$$

Measured temperatures on PCBs :

- On MANU345:

Measurement at location 1 (see Fig. 8.11) shows a raise in temperature (compared to ambiant air) of :

$$\Delta T = 10 \text{ to } 11\ ^{\circ}C$$

Measurement at location 2 (see Fig. 8.11) shows a raise in temperature (compared to ambiant air) of :

$$\Delta T = 8 \text{ to } 9\ ^{\circ}C$$

- On slat PCB :

Measurement at location 3 (see Fig. 8.12) shows a raise in temperature (compared to ambiant air) of :

$$\Delta T = 7 \text{ to } 8\ ^{\circ}C$$

Measurement at location 4 (see Fig. 8.12) shows a raise in temperature (compared to ambiant air) of :

$$\Delta T = 8\ ^{\circ}C$$

Measurement at location 5 (see Fig. 8.12), at the vertical of MANU border, shows a raise in temperature (compared to ambiant air) of :

$$\Delta T = 8 \text{ to } 9\ ^{\circ}C$$

$$\Delta T = 7 \text{ to } 8\ ^{\circ}C$$

Measurement at location 6 (see Fig. 8.13) shows a raise in temperature (compared to ambiant air) of :

$$\Delta T = 2 \text{ to } 3\ ^{\circ}C$$

Measurement at location 7 (see Fig. 8.13) shows a raise in temperature (compared to ambiant air) of :

$$\Delta T = 0 \text{ to } 1\ ^{\circ}C$$

Figure 8.11: View of a MANU345 with the measurements locations 1 and 2

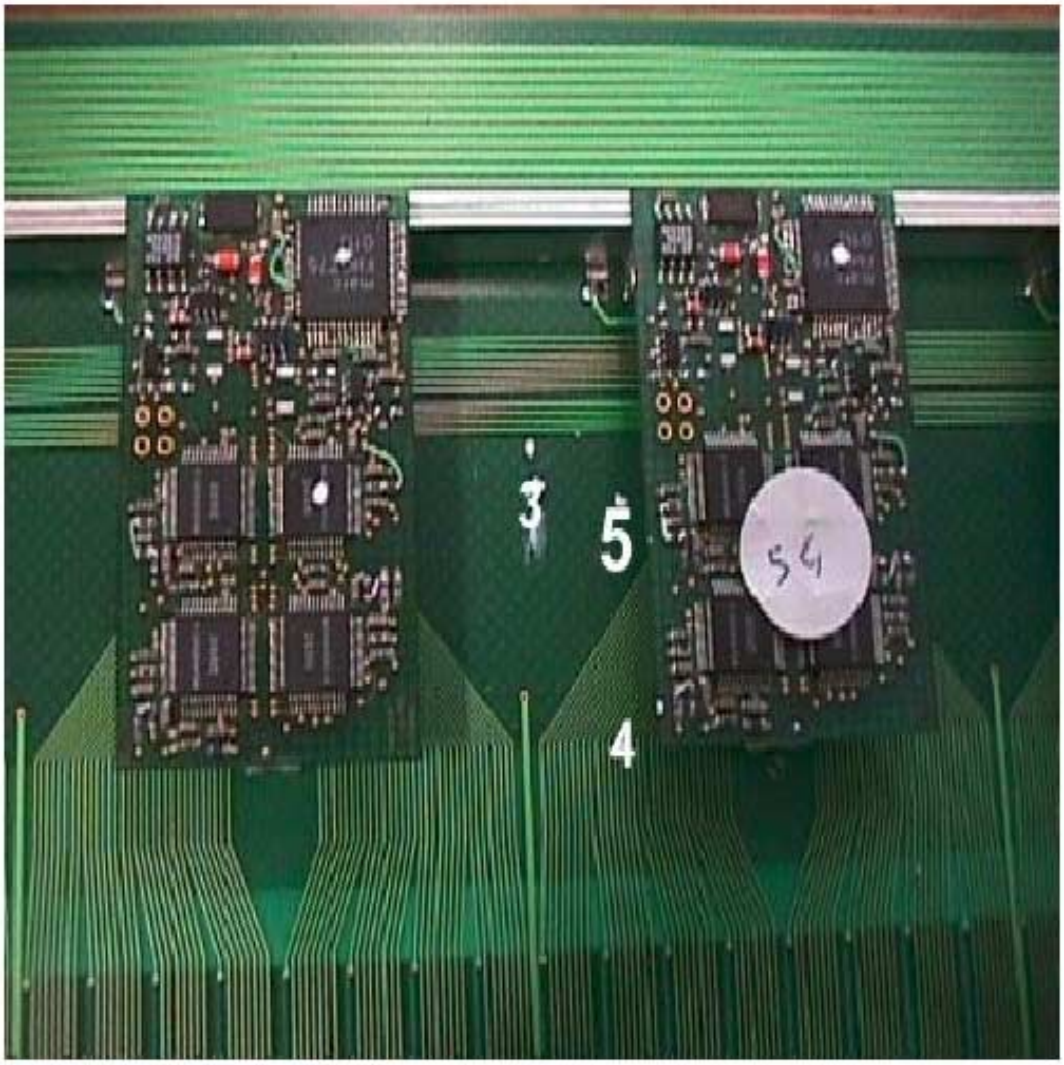

Figure 8.12: Locations (3, 4 and 5) of the measurements on the slat PCB.

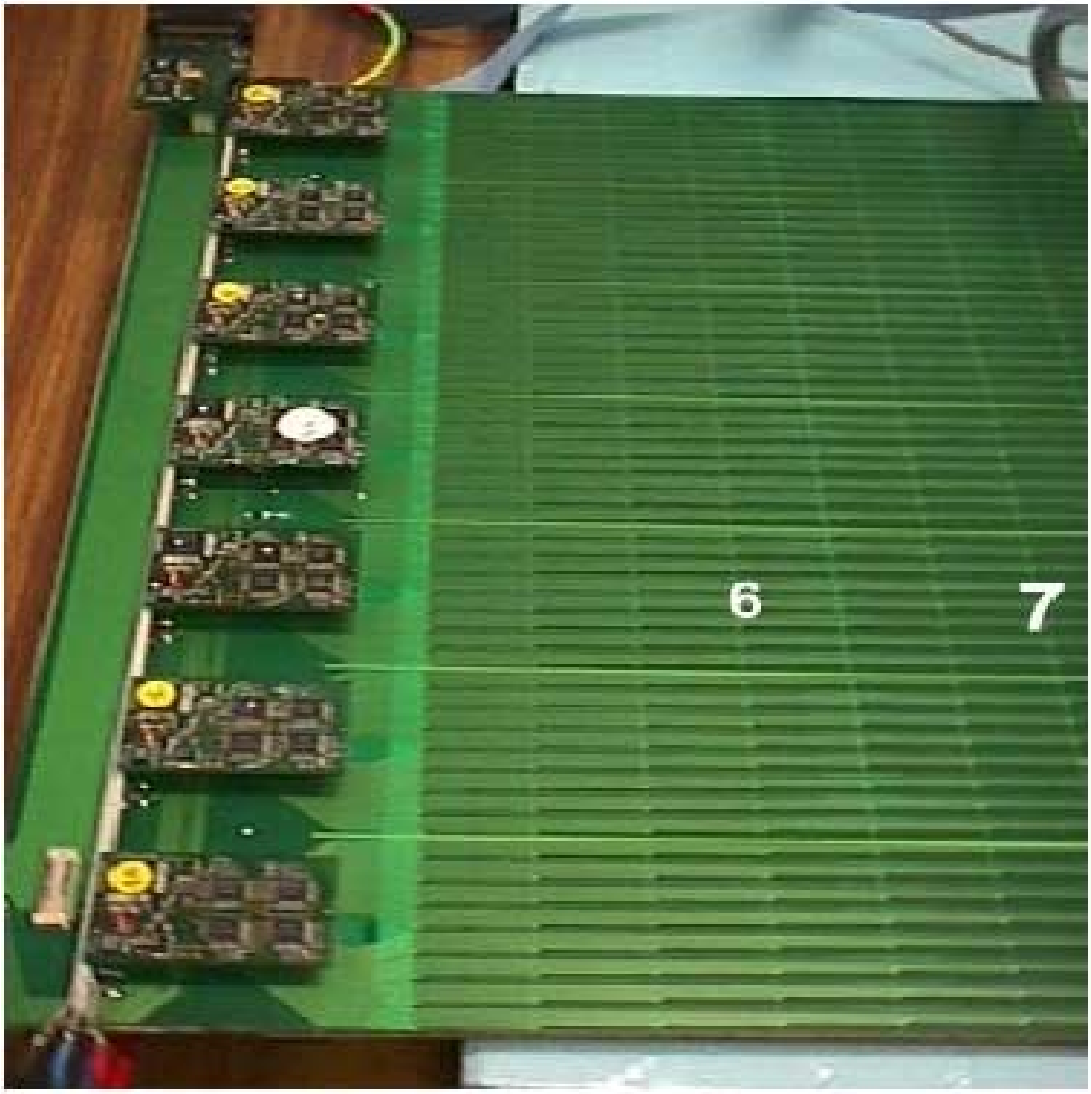

Figure 8.13: Location 6 and 7 of measurement on slat PCB.

8 Cooling (item 18)

We would like to thank the Referees for their help in our better understanding of our detectors.